Modelling and multi-objective optimization of the sulphur dioxide oxidation to the sulphur trioxide process

by

Mohammad Reza Zaker

uOttawa

Thesis submitted to the University of Ottawa
in partial Fulfillment of the requirements for the
Master of Applied Science

Department of Chemical and Biological Engineering
Faculty of Engineering
University of Ottawa

Abstract

In this thesis, the catalytic oxidation of sulphur dioxide (SO_2) to sulphur trioxide (SO_3), which is a critical step in the production of sulphuric acid (H_2SO_4), was studied under adiabatic operating conditions. The oxidation process is taking place in a heterogeneous plug flow reactor. Because the SO_2 oxidation is a highly exothermic equilibrium reaction, a series of packed bed catalytic reactors with intercooling heat exchangers is required to achieve high SO_2 conversion. To predict the effect of the operating conditions such as the temperature and the pressure on the oxidation as well as to model mathematically the reactor, it is essential to find an appropriate kinetic rate equation. In this study, various kinetic models were evaluated to select the kinetic model that appeared to be the most representative of available experimental data. In this regard, the residual sum of squares of the differences between the predicted and experimental conversion values was used to compare the various kinetic models. The model which showed the better fitting of the experimental data was the one proposed by Collina et al.

The SO_2 oxidation reactor model was developed in order to propose a methodology to perform the multi-objective optimization of many process strategies involving a number of catalytic beds and different reactor configurations. The temperature and the length of each catalytic bed are considered as decision variables to determine the optimal values of the three objectives: the SO_2 conversion, the SO_3 productivity and the catalyst weight, where the first two need to be maximized whereas the last one need to be minimized. The optimization process is comprised of two main steps. First, the Pareto domain, which contains a representative number of non-dominated solutions, was circumscribed using a non-sorting genetic algorithm. Secondly, the Pareto domain was ranked with the Net Flow method (NFM) to determine the highest-ranked Pareto-optimal solution. For ranking the Pareto domains of all strategies, a greater emphasis was placed on the SO_2 conversion because unreacted SO_2 needs to handle at the exit of the process in addition to decrease the amount of sulphuric acid produced.

Results show that the process comprised of four catalytic beds with an intermediate SO_3 absorption column provides higher SO_2 conversion in comparison with the process with four catalytic beds without an intermediate absorption column. However, the

enhanced conversion is achieved at the expense of higher operating costs. The optimum value of the total bed length for the four catalytic beds without an intermediate SO_3 absorption column commonly used industrially, is very closed to its minimum or ideal (5% difference), which clearly shows that the minimum catalyst weight almost prevails in this strategy to reach a relatively high SO_2 conversion in the vicinity of 97%.

Résumé

Dans cette thèse, l'oxydation catalytique du dioxyde de soufre (SO_2) en trioxyde de soufre (SO_3), qui est une étape critique dans la production d'acide sulfurique (H_2SO_4), a été étudiée dans des conditions opératoires adiabatiques. Le processus d'oxydation se déroule dans un réacteur hétérogène à écoulement piston. Parce que l'oxydation du SO_2 est une réaction d'équilibre hautement exothermique, une série de réacteurs catalytiques à lit garni avec des échangeurs de chaleur à refroidissement entre deux lits catalytiques successifs, est nécessaire pour obtenir une conversion élevée de SO_2. Pour prédire l'effet des conditions de fonctionnement telles que la température et la pression sur l'oxydation ainsi que pour modéliser mathématiquement le réacteur, il est essentiel de trouver une équation de vitesse cinétique appropriée. Dans cette étude, divers modèles cinétiques ont été évalués pour sélectionner le modèle cinétique qui semblait être le plus représentatif des données expérimentales disponibles. À cet égard, la somme résiduelle des carrés des différences entre les valeurs de conversion prédites et expérimentales a été utilisée pour comparer les différents modèles cinétiques. Le modèle qui montrait le meilleur ajustement des données expérimentales est celui proposé par Collina et al.

Le modèle de réacteur d'oxydation de SO_2 a été développé afin de proposer une méthodologie pour effectuer l'optimisation multi-objectif de nombreuses stratégies de procédé impliquant un certain nombre de lits catalytiques et différentes configurations de réacteur. La température et la longueur de chaque lit catalytique sont considérées comme des variables de décision pour déterminer les valeurs optimales des trois objectifs: la conversion du SO_2, la productivité du SO_3 et le poids du catalyseur, où les deux premiers doivent être maximisés tandis que le dernier doit être minimisé. Le processus d'optimisation comprend deux étapes principales. Tout d'abord, le domaine de Pareto, qui contient un nombre représentatif de solutions non dominées, a été circonscrit à l'aide d'un algorithme génétique. Deuxièmement, le domaine Pareto a été classé avec la méthode Net Flow (NFM) pour déterminer la solution optimale de Pareto la mieux classée. Pour classer les domaines Pareto de toutes les stratégies, une plus grande importance a été accordée à la conversion du SO_2 car le SO_2 n'ayant pas réagi doit être traité à la sortie du processus, en plus de diminuer la quantité d'acide sulfurique produite.

Les résultats montrent que le procédé comprenant quatre lits catalytiques avec une colonne d'absorption intermédiaire de SO_3 fournit une conversion plus élevée de SO_2 par rapport au procédé avec quatre lits catalytiques sans colonne d'absorption intermédiaire. Cependant, la conversion améliorée est obtenue au détriment de coûts d'exploitation plus élevés. La valeur optimale de la longueur totale du lit pour les quatre lits catalytiques sans colonne intermédiaire d'absorption de SO_3 couramment utilisée industriellement, est très proche de son minimum (différence de 5%), ce qui montre clairement que le poids minimum du catalyseur prévaut presque dans cette stratégie pour atteindre une conversion de SO_2 relativement élevée aux alentours de 97%.

Statement of Contributions

I hereby declare that this work has not been submitted or accepted for any other degree. Dr. Jules Thibault and Dr. Clémence Fauteux-Lefebvre supervised the research performed in this thesis.

Chapter 2, entitled “Kinetic models and operating conditions for the sulphur dioxide oxidation with a vanadium catalyst“, was thoroughly suggested by me. I proposed using empirical models and performed all analysis. I wrote the first draft of the paper and made numerous revisions based on the comments from my two supervisors.

Chapter 3, entitled “Modelling and multi-objective optimization of the sulphur dioxide oxidation process“ was proposed by me. The idea of solving the multi-objective optimization problem with the finite difference method was suggested by me. The finite difference method was initially coded by Dr. Jules Thibault in the FORTRAN, then further developed by me. I performed many simulations and wrote the first draft of the paper. The draft was revised by me with constructive comments from my supervisors.

Acknowledgments

First and foremost, I would like to express my deep gratitude to my supervisor, Dr. Jules Thibault who was the most patient and supportive professor one could ask during this research. I will always be grateful to him for sharing his knowledge with me and for helping me along the way. I would also like to express my sincere gratitude to Dr. Clémence Fauteux-Lefebvre, who co-supervised this work and provided me with her insight on chemical reactors and catalysis. I would not have been able to complete this thesis without their continuous support, insights and invaluable guidance.

I would also want to thank my family and friends for their encouragement and support that made this research journey an unforgettable experience.

I would like to acknowledge the Natural Science and Engineering Research Council (NSERC) of Canada for providing the financial support for this work.

Table of Contents

List of Figures

List of Tables

Chapter 1. Introduction

1.1 Introduction

The catalytic oxidation of sulphur dioxide (SO_2) to sulphur trioxide (SO_3) is a key step in the sulphuric acid (H_2SO_4) production by providing the SO_3 required for subsequent H_2SO_4 making. Sulphuric acid has been considered as a strong mineral acid[1] which is an essential commercial chemical that is used in the production processes of many commodities over a wide range of applications such as fertilizer, metal processing, petroleum refining, lead-acid batteries and medical processes[2]. Sulphuric acid manufacturing has attracted significant interest during the past decades and it can be produced mainly in two ways: lead chamber process and contact process[3]. The lead chamber process has been mostly replaced by the contact process in more modern industrial plants because of the small plant size and relatively dilute acid production (62 - 78% H_2SO_4) of the chamber process[4]. The contact process produces a more concentrated acid but requires pure raw materials and the use of catalysts[5]. The contact process consists of three main steps. In the first step, elemental sulphur (S) is completely combusted to form sulphur dioxide (SO_2) in the presence of excess dry air in the furnace. SO_2 is then oxidized to sulphur trioxide (SO_3) in a series of large adiabatic catalytic packed bed reactors. Finally, sulphur trioxide is absorbed in an absorption column with concentrated sulphuric acid where it reacts with water to produce additional sulphuric acid[1]. The critical step in sulphuric acid production is the oxidation of SO_2 to SO_3 which is a highly exothermic equilibrium reaction. The reactor is operated as a plug flow reactor under adiabatic conditions. The oxidation is carried out in multi-catalytic beds with gas cooling between adjacent beds to decrease the temperature of the gas mixture prior to entering the next catalytic bed[1].

Catalyst obviously plays an important role in the oxidation of SO_2 to SO_3. The commercial catalyst currently used industrially for the SO_2 oxidation to SO_3 is vanadium pentoxide (V_2O_5) which provides high activity and low-pressure drop along

each catalytic bed[6]. It can be used with different composition of alkali metals such as Na, K and Rb as a promoter because V_2O_5 is considered to be a weak catalyst on its own. The catalyst has a minimum required temperature of about 400°C to launch a self-sustaining reaction, which is known as a strike temperature of catalyst. Research is currently conducted to find ways to reduce the strike temperature of catalyst such as using cesium as a promoter.

The oxidation of sulphur dioxide has been studied for many decades and numerous attempts have been undertaken to find a proper kinetic model that will faithfully represent industrial data and elucidate the chemical reaction mechanism and interaction with the catalyst. Some of the more popular models are those that were proposed by Collina et al.[7], Calderbank[8], Villadsen et al.[9], and Eklund[10].

Because of the complexity of the SO_2 to SO_3 reactor configuration, it is important to operate under optimal conditions. It is clearly paramount to maximize the SO_2 oxidation conversion, as unreacted SO_2 will need to be removed following the SO_3 absorption tower. However, a high conversion should not be achieved at the expense of very low SO_3 productivity and a large reactor volume. Indeed, it is also desire to maximize the productivity and minimize the reactor volume, Therefore, to resolve these conflicting objectives, a multi-objective optimization (MOO) can be used to strike a compromise between the various objectives that would be satisfactory in the eye of the decision-maker. This work therefore resorts to a MOO algorithm to investigate the impact of the number of catalytic packed beds and the addition of an intermediate absorption column for conducting this oxidation reaction. The MOO algorithm allows comparing the optimal solution of each studied strategies on the basis of various process objectives.

The subject of this thesis is mainly focused on two aspects. The first one is to repertory the various kinetic equations describing the conversion of SO_2 to SO_3 that are applicable for sulphuric acid plants, and to investigate the impact of various operating parameters on the oxidation reaction. Then, an experimental design was used to select the most appropriate kinetic equation, which best represents the experimental data. To select the most representative kinetic equation, the residual sum of squares (RSS) of the differences between the predicted and experimental data

in the range of temperature of interest was minimized. The most appropriate kinetic model shows a wide range of validity or the lowest average of RSS value in comparison with other kinetic models.

The second part of this thesis is focused on performing a multi-objective optimization study on the oxidation of SO_2 to SO_3 for series of strategies involving a good number of catalytic beds and reactor configurations of the multi-bed catalytic reactor in order to determine the optimal operating conditions leading to solutions that represent a suitable compromise among all the objectives. Multi-objective optimization (MOO) refers to the process of systematically and simultaneously optimize a collection of conflicting functions[11]. This type of optimization generates a set of alternative solutions, called the Pareto-domain which only contains solutions that are non-dominated[12]. The optimization problem in this study includes the temperature and the length of each catalytic bed as the set of decision or input variables that can be used to optimize three partly conflicting objectives (the conversion of SO_2, the productivity of SO_3, the catalyst weight). In order to carry out a MOO for the oxidation of SO_2 to SO_3, a mathematical model of the complete packed bed catalytic reactor was used. The model is comprised of the kinetic rate equation, the mass balance of a plug flow design equation to follow the progression of the reaction, an energy balance to track the temperature along the packed bed, and the Ergun equation to account for the pressure of the reacting mixture. The optimization process includes two main steps. First, the Pareto-domain is circumscribed by generating a very large number of feasible solutions via non-sorting genetic algorithm II (NSGA-II)[13]. The Pareto domain is obtained without introducing any bias with respect to preferences of a decision-maker. However, to rank all Pareto-optimal solutions, it is required to capture in one way or another the preferences of an expert into the selection of the best Pareto-optimal solution. In this investigation, the Net Flow method will be used to rank all solutions pertaining to the Pareto domain where the a priori knowledge of the process expressed by the decision-maker is incorporated into the optimization routine using four sets of ranking parameters[11].

1.2 Research objectives

The main objectives of this thesis are:

1. To select an appropriate kinetic equation, among the numerous kinetic rate equations published in the literature, to represent the experimental data for the SO_2 oxidation to SO_3. This research was also interested in evaluating the range of validity for each kinetic model.
2. To perform the multi-objective optimization of the oxidation of SO_2 to SO_3 in the multi-bed catalytic reactor for a different number of catalytic beds and reactor configurations, in order to determine the optimal values of input or decision variables (temperature and length of each bed) that lead to the most suitable compromise among all considered objectives (the SO_2 conversion, the SO_3 productivity, the catalyst weight).

1.3 Thesis structure

This thesis consists of four chapters. The first chapter presents a general introduction to the oxidation of sulphur dioxide to sulphur trioxide and the different research objectives that were considered during the course of this research. Chapter 2 presents a study on the oxidation of SO_2 to SO_3 in view of selecting an appropriate kinetic equation to represent experimental data. Chapter 3 presents the modelling and multi-objective optimization of SO_2 oxidation to SO_3 in the multi-bed catalytic reactor, in order to identify the optimal output of the reactor and their respective operating conditions. Chapters 2 and 3 were written in the format of a paper and they will be submitted to scientific refereed journals. Due to the paper-based structure, it is possible and inevitable to find that some concepts will be repeated through this work. As for Chapter 4, it contains a general discussion tackling the main conclusions and recommendations based on the work that was performed in this thesis.

References

1. King, M. J., Davenport, W. G. & Moats, M. S. Overview. in Sulfuric Acid Manufacture Elsevier, pp 1–9, (2013).
2. Kiss, A., S.Bildea, C. & Grievink, J. Dynamic modeling and process optimization of an industrial sulfuric acid plant. Chem. Eng. J. 158, pp 241–249 (2010).
3. Schöneberger, J. C., Arellano-Garcia, H., Wozny, G., Körkel, S. & Thielert, H. Model-based experimental analysis of a fixed-bed reactor for catalytic SO_2 oxidation. Ind. Eng. Chem. Res. 48, pp 5165–5176 (2009).
4. Ashar, N. G. & Golwalkar, K. R. A Practical Guide to the Manufacture of Sulfuric Acid, Oleums, and Sulfonating Agents. in Processes of Manufacture of Sulfuric Acid, Springer, Cham, pp 5-10 (2013).
5. Benzinger, W., Wenka, A. & Dittmeyer, R. Kinetic modelling of the SO_2-oxidation with Pt in a microstructured reactor. Appl. Catal. A Gen. 397, pp 209–217 (2011).
6. Doering, F. J., Unland, M. L. & Berkel, D. A. Modelling of SO_2 oxidation rates based on kinetic data of a Cs/V catalyst at high pressures and conversions. Chem. Eng. Sci. 45, pp 1939–1941 (1988).
7. Collina, A., Corbetta, D., and Cappelli, A., "Use of Computers in the Design of Chemical Plants", in Proc. Eur. Symp, Firenze, pp 329 (1971).
8. Calderbank, P H. The mechanism of the catalytic oxidation of sulphur dioxide with a commercial vanadium catalyst: A kinetic study. J. App. Chem.; pp 482-492 (1952)
9. Villadsen, J. & Livbjerg, H., Kinetics and effectiveness factor for SO_2 oxidation on an industrial vanadium catalyst. Chem. Eng. Sci. 27, pp 21–38 (1972).
10. Eklund, R. B., Dissertation in the Manufacture of Sulfuric, Royal Institute of Technology, Stockholm, pp. 166–168. (1956)
11. Thibault, J., Lanouette, R., Fonteix, C. & Kiss, L. N. Multicriteria Optimization of a High-Yield Pulping Process. Can. J. Chem. Eng. 80, pp 897–902 (2008).
12. Bineli, A., Thibault, J., Jardini, A. & Filho, R. M. Ethanol steam reforming for hydrogen production in microchannel reactors: Experimental design and optimization. Int. J. Chem. React. Eng. 11, pp 9–17 (2013).
13. Raghuwanshi, M. M. & Kakde, O. G. Survey on multiobjective evolutionary and real

coded genetic algorithms. Complex. Int. pp 150–161 (2004).

Chapter 2.

Kinetic models and operating conditions for the sulphur dioxide oxidation with a vanadium catalyst

Mohammad Reza Zaker, Jules Thibault, Clémence Fauteux-Lefebvre
Department of Chemical and Biological Engineering
University of Ottawa
Ottawa, Ontario, Canada K1N 6N5

Abstract

The critical step in the sulphuric acid production is the catalytic oxidation of sulphur dioxide to sulphur trioxide, which a highly exothermic equilibrium reaction. The common industrial catalyst for this reaction is vanadium pentoxide (V_2O_5) with alkali metals (Na, K) as promoters, which provides high activity and low-pressure drop. This paper investigates the effect of the operating conditions such as the feed gas composition and pressure on the equilibrium oxidation. It is paramount to identify the most representative kinetic rate equation in order to predict the effect of operating conditions and to develop a mathematical model of the SO_2 oxidation, which occurs along a multi-bed catalytic reactor.

In this investigation, many kinetic rate equations were considered, all based on the vanadium pentoxide catalyst, to assess their ability to represent the experimental kinetic data over a wide range of operating conditions. A total of 135 data points obtained from the literature were used to assess the range of validity of each kinetic model. Based on the residual sum squares of the difference between the predicted and experimental data, it is shown that the model proposed by Collina et al. was the one showing the best predictions.

2.1 Introduction

Sulphuric acid (H_2SO_4) is an important chemical, used primarily in the production of fertilizer, but also in myriad of material fabrication processes[1]. Figure 2-1(b) shows the usage of sulphuric acid in various industrial sectors such as fertilizer, metal processing and medicine manufacturing[1] The worldwide annual production of sulphuric acid in 2017 is over 200 million tonnes[2]. China has the highest production rate with 74 million tones of H_2SO_4 produced per year (Figure 2-1a)[2]. Canada has appeared as one of the top H_2SO_4 suppliers in the world since 2016, exporting around 85,000 tonnes of H_2SO_4 (corresponding to a value of over US $104 million) annually[2].

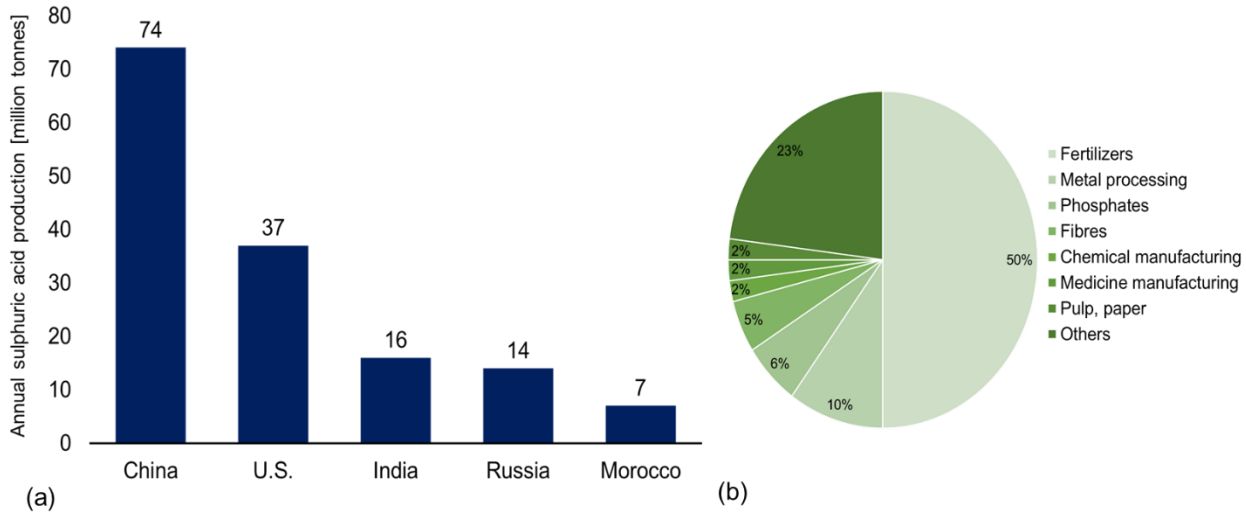

Figure 2-1(a) Worldwide sulphuric acid production (b) Usage of the sulphuric acid. Adopted from Sulphuric acid manufacture book[2]

Sulphuric acid has been historically produced by different processes such as the contact process, wet contact, lead chamber and hydrogen peroxide. The contact process is today the leading technology used in the manufacture of sulphuric acid because of its large production capacity of concentrated sulphuric acid compared to all the other processes. This process consists of three main reactions carried in different units: 1) elemental sulphur is burned with air to produce sulphur dioxide (SO_2) (Eq. 22); 2) the sulphur dioxide is oxidized to sulphur trioxide (SO_3) using oxygen (O_2) from the air (Eq. 23); (3) the sulphur trioxide is absorbed in a concentrated sulphuric acid column where

SO_3 reacts with water to form additional H_2SO_4 (Eq. 3). The three steps are exothermic. The second step is the critical step in sulphuric acid production mainly because SO_2 oxidation to SO_3 is an exothermic and equilibrium reaction performed adiabatically such that a multi-bed catalytic reactor is required to achieve a high conversion.

$$S_{(s)} + O_{2\,(g)} \rightarrow SO_{2\,(g)} \qquad \Delta H_R = -296\,810\ [\frac{kJ}{kmol}] \tag{1}$$

$$SO_{2\,(g)} + 0.5\ O_{2\,(g)} \leftrightarrow SO_{3\,(g)} \qquad \Delta H_R = -96\,232\ [\frac{kJ}{kmol}] \tag{2}$$

$$SO_{3\,(g)} + H_2O_{(l)} \rightarrow H_2SO_{4\,(l)} \qquad \Delta H_R = -132\,000\ [\frac{kJ}{kmol}] \tag{3}$$

The SO_2 oxidation process is very important in terms of capital investment and operating costs, as well as for its needs for optimization and control. It is an equilibrium catalytic reaction, generally carried out in plug flow reactors under adiabatic conditions. Industrially, a series of three to five catalytic beds are used to perform this reaction with inter-stage gas-cooling. A schematic diagram of a four bed catalytic converter is presented in Figure 2-2. The typical length of individual catalytic packed beds ranges between 0.2 and 2.0 m, with diameters up to 12 m. Removing heat from the reacting gas mixture between catalyst beds needs to be performed to increase the conversion.

The conventional contact method is a very effective process for making H_2SO_4 in view of the conversion of SO_2 to SO_3 (achieving 97.5% conversion). It can be further improved by 1 to 2 % by using two stages of sulphur trioxide absorption columns (double contact method). An intermediate absorption column is incorporated between two catalytic beds to recover SO_3 and enhance additional conversion. However, this higher conversion is obtained at the expense of a much larger amount of catalyst and additional process equipment such as extra heat-exchangers and an absorption column which increase both the capital and operating expenses.

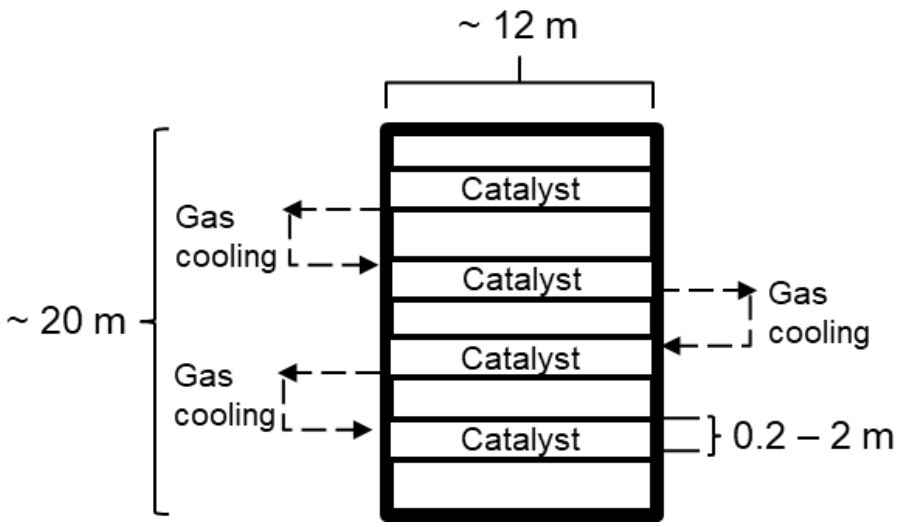

Figure 2-2 Simplified schematic flowsheet of a typical industrial SO_2 oxidation converter with four fixed catalyst bed reactors. The total height of the converter can reach be 20 m with the four 12 m diameter and 0.2 to 2 m long catalyst beds.

To properly study, control and optimize the multi-bed oxidation catalytic reactor for the SO_2 to SO_3 reaction is to identify a representative and reliable kinetic rate equation that is able to predict accurately the fate of reacting molecules for the range of experimental conditions encountered in an industrial reactor. Such model is very useful for the optimization of the process by identifying the optimal operating conditions that lead to the best process performance metrics. For the SO_2 oxidation on vanadium pentoxide (V_2O_5) catalyst, a number of kinetic models have been proposed but each one was obtained over a limited range of operating conditions. Various model evaluation techniques can be used under the supervised learning setup that helps us in finding how good our model is performing. A very simple method to evaluate a model is by finding the accuracy which is the difference between the predicted and actual values, however, it is not a perfect method and can lead to poor decision making. Therefore, we need other measures to evaluate the various models and picking the right measure of evaluation is crucial in selecting and distinguishing the right model from other models. Thus, the method of the residual sum squares (RSS) is often used to measure the discrepancy between the data and a kinetic model and assess which model will best predict experimental data in the range of interest.

2.1.1 Catalysts

The sulphur dioxide (SO_2) oxidation to the sulphur trioxide (SO_3) is a heterogeneous catalytic reaction. In the beginning, platinum catalysts were used because they have high activity for this reaction. However, platinum is very costly and is easily deactivated by many trace materials such as arsenic trioxide (As_2O_3)[3]. Development of the contact process led to the use of alternative catalyst, such as vanadium pentoxide (V_2O_5), having a longer lifetime and being significantly cheaper to manufacture[3], V_2O_5 combined with alkali metal oxide promoters form the active phase of the catalyst, which is typically added to porous silica as the support[4]. The main alkali metal sulphate promoters used are Na_2SO_4, K_2SO_4, Rb_2SO_4[5] and showed to enhance the efficiency of the catalysts. A composition of 1 mol V_2O_5 with 2.5 moles of alkali metal sulphate is typically used in many industrial vanadium catalysts[6].

The overall concentration of V_2O_5 generally ranges from 5 to 7 wt% for the standard V_2O_5 catalysts and from 7 to 9% for high-V_2O_5 catalysts. The catalyst activity was shown to be improved by 10% with the one having the highest concentration[7]. The catalyst activity can also be reduced by feed gas impurities, which in turn affects the SO_2 oxidation conversion[8]. Chloride causes vanadium loss and reduction in catalyst activity. Fluoride attacks the catalyst carrier whereas iron oxide and dust will progressively plug the catalyst bed causing an increase in pressure drop[8]. For this is the reason, the sulphuric acid manufacturing process usually uses few cleaning columns to remove undesirable impurities and prolong the life of the catalyst. Active research is currently under way to find a better catalyst or a way to remove more effectively the detrimental trace elements, such as removing dust by electrostatic precipitation and aqueous scrubbing.

V_2O_5–alkali catalyst shows high catalytic activity and stability for temperature ranging from 420˚C to 560˚C[4]. The minimum temperature at which the catalyst promotes the sulphur dioxide oxidation is called the catalyst strike or auto-ignition temperature[9]. The standard V_2O_5–alkali catalysts have a strike temperature of about 420˚C[10]. The use of cesium (Cs) as a promoter, has shown that the strike temperature can be decreased by 20 to 40˚C [11] with reasonable catalyst activity, which has a significant impact on the process design of the oxidation reactor. The catalyst improvement will allow the plant to operate at a lower inlet gas temperature, effectively reducing the auto-thermal limitation

of the plant without increasing the size of the heat exchangers[2]. At a usual inlet temperature of 420˚C, the resulting outlet temperature would be higher than 650˚C which would exceed the typical design temperature of a stainless-steel converter[12]. Lowering the inlet temperature to 390˚C results in an outlet temperature of 635˚C with the same conversion. The further advantage of cesium promoted catalyst could be in the double contact acid making where the gas coming from the intermediate acid-making column must be reheated back to the converter. In this situation, using a cesium-promoted catalyst for the bed following the intermediate acid-making column, it would be possible to operate at lower inlet temperatures and effectively increasing the room for additional conversion to occur[5].

Industrial catalysts come in different shapes and forms with the motivation to reduce the pressure drop along each catalytic bed in the oxidation of SO_2 to SO_3 without compromising on the catalyst activity or the mechanical strength[10]. Initially, V_2O_5 catalysts were manufactured as cylindrical pellets. However, ring-shaped catalysts provide a pressure drop reduction of up to 50% over pellet-shaped catalyst[4]. By increasing the ring size, it is possible to provide an even bigger reduction in pressure drop and are worth using in special situations where rapid dust builds up in the bed can occur[6]. Ribbed or daisy-shaped rings are a further improvement on the standard rings. The ribs on the outside of the ring increase the surface area which provides more contact area for the gas mixture to migrate into the catalyst pores[10]. The present catalyst shape (BASF Quattro shape) has four internal holes that cause more of the catalyst internals available for the sulphur dioxide oxidation[3].

2.1.2 Finding the appropriate kinetic model

To study the reaction kinetics of SO_2 oxidation to SO_3, the kinetic results obtained from experimental design which was proposed by Doering et al.[13], were used while considering some important aspects. One aspect is the choice of catalysts was the same for both the kinetic rate equations and the experimental data. Further, the experimental data can be affected by some outliers, arising from experimental errors, incorrect data management or model inadequacy. These outliers must be identified prior to the model

evaluation; otherwise, estimation errors may occur since the method of residual sum squares (RSS) often fails in identifying outliers.

This investigation aims to select a representative kinetic model to explain adequately the experimental data. Four kinetic models were identified from the literature review based on the V_2O_5 catalyst. Then, the residual sum squares (RSS) of the differences between the predicted and experimental data was used to assess the model validity over different ranges of operating conditions.

2.2 Mechanisms and rate laws

There are two main hypothetical reaction mechanisms that were proposed to explain the observed experimental data on the alkali-V_2O_5 catalyst under certain operating conditions[13]. Calderbank[14] and Eklund[15] suggested a two-step mechanism: (1) vanadium components oxidize the sulphur dioxide to the sulphur trioxide, and (2) oxygen re-oxidizes V^{+4} to V^{+5} (Eq.(4)-(5)). The degree of vanadium reduction in the first step was measured based on the quantity value of $\frac{[V^{+4}]^2 \cdot P_{SO_3}}{[V^{+5}]^2 \cdot P_{SO_2}}$ over a large range of reaction conditions and catalyst composition[8]. Calderbank was assumed that the vanadium reduction (step 2) was rate-determining[8] (Eq. (5)) and derived a kinetic model (Eq.(6)). Eklund[15] worked on the same mechanism and proposed a different kinetic model that represented experimental results more accurately. His model includes an equilibrium constant (Eq.(7)). However, this equation can only be used when the SO_2 conversion is greater than 5%. For conversion lower than 5%, the rate reaction is the one that prevails for 5% conversion[15].

$$SO_2 + 2V^{5+}O^{2-} \rightleftarrows SO_3 + 2V^{4+} \tag{4}$$

$$2V^{4+} + 0.5O_2 \rightleftarrows 2V^{5+} + O^{2-} \tag{5}$$

$$-r_{SO_2} = \frac{k_1 p_{O_2} p_{SO_2} - k_2 p_{SO_3} p_{O_2}^{0.5}}{p_{SO_2}^{0.5}} \ \left[\frac{kmol}{kg_{cat} \cdot s}\right] \tag{6}$$

$$-r_{SO_2} = k_1\left(\frac{p_{SO_2}}{p_{SO_3}}\right)^{0.5}\left[p_{O_2} - \left(\frac{p_{SO_3}}{K_p . p_{SO_2}}\right)^2\right] \left[\frac{kmol}{kg_{cat} \cdot s}\right] \quad (7)$$

The parameters of the kinetic rate equations are given in Table 2-1.

Ivanenko et al.[16] proposed a three-step reaction mechanism. However, they did not provide a kinetic rate equation to properly explain and support the experimental data. Villadsen and Livbjerg[17] worked on the same mechanism which involving: (1) vanadium components oxidize the SO_2 and produce a $[V^{+4}.SO_3]$ complex, (2) the complex dissociates into SO_3 and V^{+4}, and (3) the V^{+4} reoxidizes to V^{+5} (Eq.(8)-(10)). Villadsen et al. assumed that the oxidation of V^{4+} species (step 3) is a crucial step (Eq.(10)) in the oxidation of SO_2 to SO_3 and they derived a kinetic equation to explain their experimental results[13] (Eq.(11))).

$$2V^{5+} + SO_2 \rightleftarrows 2V^{4+}.SO_3 \quad (8)$$

$$2V^{4+}.SO_3 \rightleftarrows 2V^{4+} + SO_3 \quad (9)$$

$$2V^{4+} + 0.5O_2 \rightleftarrows 2V^{5+} \quad (10)$$

$$-r_{SO_2} = \frac{k_1 \cdot p_{O_2}^{0.5} \cdot \left(1 - \frac{p_{SO_3}}{K_p \cdot p_{SO_2} \cdot p_{O_2}^{0.5}}\right)}{K_2 + K_3 \cdot p_{SO_3} + \frac{p_{SO_3}}{p_{SO_2}}} \left[\frac{kmol}{kg_{cat} \cdot s}\right] \quad (11)$$

Collina et al.[18]proposed a kinetic rate equation (Eq.(12)) based on the Hougen-Watson concept and on the assumption that the reaction between adsorbed SO_2 and O_2 from the gas phase is the rate-controlling step[18]. In addition, the rate equation properly explains their experimental data for a temperature range of 420-590°C.

$$-r_{SO_2} = \frac{k_1 \cdot p_{O_2} \cdot p_{SO_2}\left(1 - \frac{p_{SO_3}}{K_p \cdot p_{SO_2} \cdot p_{O_2}^{0.5}}\right)}{22.414(1 + K_2 \cdot p_{SO_2} + K_3 \cdot p_{SO_3})^2} \left[\frac{kmol}{kg_{cat} \cdot s}\right] \quad (12)$$

The parameters of kinetic rate expressions (Eq.(11)) and(12)) are presented in Table 2-1.

Table 2-1 Kinetic parameters and ranges of operating variables.

Parameters	**Temperature dependence**	**T [˚C]**
Model 1: Collina et al.[18]		
k_1 [kmol/kg_{cat} · atm^2 · s]	k_1 = exp (12.16 - 5473/T)	
K_2 [atm^{-1}]	K_2 = exp (-9.953 + 8619/T)	420 - 590
K_3 [atm^{-1}]	K_3 = exp (-71.745 + 52596/T)	
K_P [$atm^{-0.5}$]	K_P = exp (-10.68 + 11300/T)	
Model 2: Eklund[15]		
k_1 [kmol/kg_{cat} · atm · s]	k_1 = exp (848.14 – 97782.2/T – 110.1 lnT)	420 - 554
K_P [$atm^{-0.5}$]	K_p = exp (-11.24 + 11818.055/T)	
Model 3: Calderbank[14]		
k_1 [kmol/kg_{cat} · $atm^{1.5}$ · s]	k_1 = exp (12.07 - 15656.56/T)	370 - 450
k_2 [kmol/kg_{cat} · atm · s]	k_2 = exp (22.75 – 27070.7/T)	
Model 4: Villadsen et al.[17]		
k_1 [kmol/kg_{cat} · atm · s]	k_1 = exp (-1.88 – 7466.08/T)	
K_2 [-]	K_2 = exp (2.10 – 286.74/T)	380 - 520
K_3 [atm^{-1}]	K_3 = exp (-1.51 + 2279.17/T)	
K_P [$atm^{-0.5}$]	K_P = exp (-10.73 + 11318.3/T)	

2.3 Equilibrium curve

The oxidation of SO_2 to SO_3 is an equilibrium reaction, which dictates the maximum conversion that can be achieved given the operating conditions. Therefore, it is important to define accurately the equilibrium curve. The chemical reaction reaches equilibrium

when the forward and backward reaction rates are equal such that the net reaction rate is zero and both reactants and products remains at the same concentration[2]. The equilibrium curve is independent of the catalyst and kinetics of reaction. It is a function of concentration, pressure and temperature. The maximum SO_2 oxidation conversion for a given adiabatic catalytic bed is achieved when the reaction comes to equilibrium[15]. The equilibrium equation for SO_2 oxidation is given in Equation (13).

$$K_p = \frac{p_{SO_3}}{p_{SO_2} \cdot p_{O_2}^{0.5}} \tag{13}$$

The temperature-dependent equilibrium constant of the SO_2 to SO_3 reaction is given in Eq. (14)[18]:

$$K_P = \exp\left(\frac{11300}{T} - 10.68\right) \tag{14}$$

Knowing that the partial pressures p_{SO_2}, p_{O_2}, and p_{SO_3} in Eq. (13) are related to feed gas compositions and the current conversion, their current values are determined using Eqs. (15), (16), and (17), respectively.

$$p_{SO_2} = \frac{y_{SO_2} - 0.01 \cdot y_{SO_2} \cdot X}{100 - 0.005 \cdot y_{SO_2} \cdot X} \times P_t \tag{15}$$

$$p_{O_2} = \frac{y_{O_2} - 0.005 \cdot y_{SO_2} \cdot X}{100 - 0.005 \cdot y_{SO_2} \cdot X} \times P_t \tag{16}$$

$$p_{SO_3} = \frac{0.01 \cdot y_{SO_2} \cdot X}{100 - 0.005 \cdot y_{SO_2} \cdot X} \times P_t \tag{17}$$

Equation (13) can be rewritten as Eq. (18), in terms of feed gas compositions and conversion.

$$K_P = \frac{X(100 - 0.005 \cdot y_{SO_2} \cdot X)^{0.5}}{(100 - X)(y_{O_2} - 0.01 \cdot y_{SO_2} \cdot X)^{0.5}} \times P_t^{-0.5} \quad (18)$$

The equilibrium temperature is then related to the equilibrium conversion by combining Eqs. (14) and (18) to give Eq. (19).

$$T = \frac{11300}{10.68 + \ln\left(\frac{X(100 - 0.005 \cdot y_{SO_2} \cdot X)^{0.5}}{(100 - X)(y_{O_2} - 0.01 \cdot y_{SO_2} \cdot X)^{0.5}} \times P_t^{-0.5}\right)} \quad (19)$$

Figure 2-3 presents the plots Eq. (19) for different equilibrium total pressures for the feed gas composition of 10 mol% SO_2, and 11 mol% O_2, and 79 mol% N_2. Figure 2-3 emphasizes that the conversion increases with decreasing the equilibrium temperature. In addition, an increase in pressure allows a higher conversion at a given temperature. As expected, due to the Le Chatelier's principle, increasing the pressure favours the forward reaction as it reduces the total number of moles.

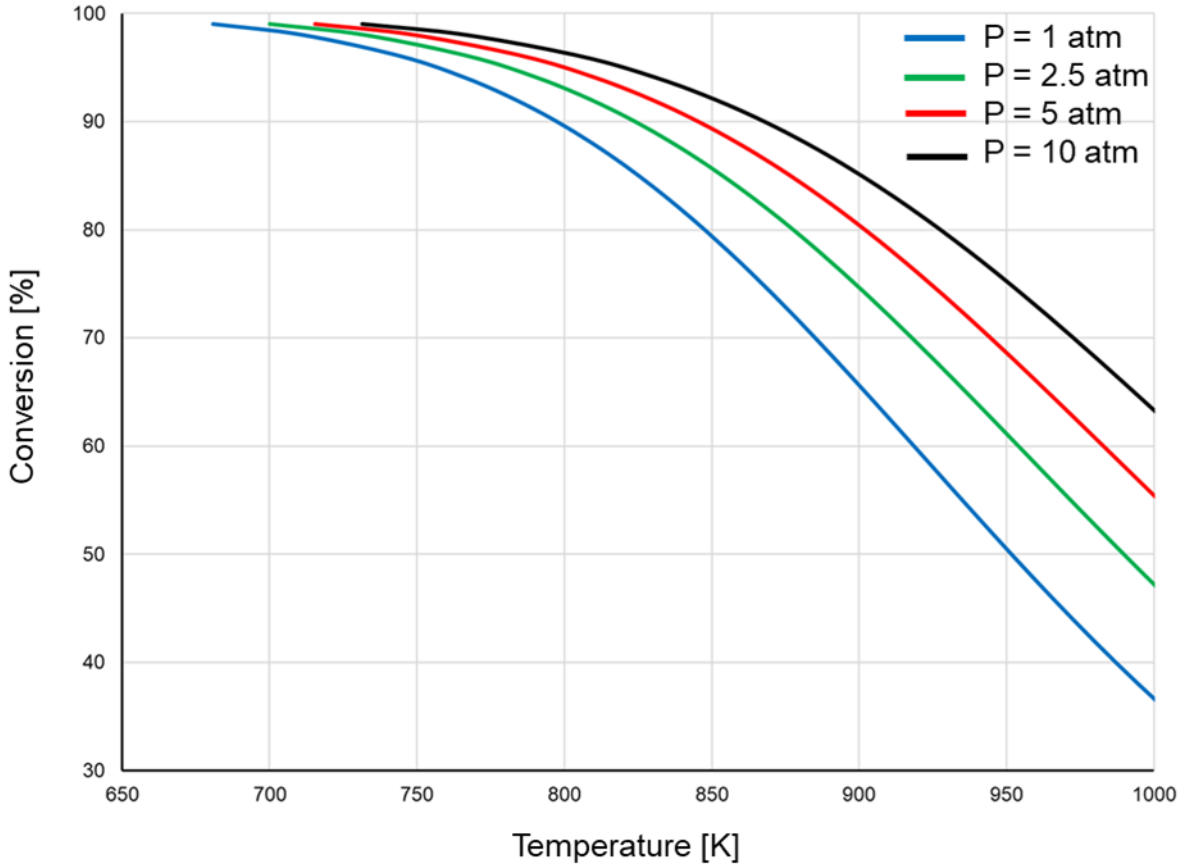

Figure 2-3 Equilibrium sulphur dioxide oxidation curve as a function of temperature for different total pressures and feed gas composition (10% SO_2, 11% O_2, 79% N_2).

2.3.1 Influence of SO_2 and O_2 concentrations in feed gas

Figure 2-4 shows the effect of the mole fraction of O_2 and SO_2 in feed gas mixture on the equilibrium conversion as a function of the temperature for the SO_2 oxidation at a total pressure of one atm. The feed gas composition entering the reactor depends on the amount of air used in furnace to combust elemental sulphur. Decreasing the air/sulphur ratio decreases the O_2/SO_2 ratio of the inlet reactor gas stream, potentially lowering catalytic SO_2 oxidation conversion. Results of Figure 5(a) are plotted for a constant SO_2 concentration whereas results for Figure 5(b) are for a constant O_2/SO_2 ratio and different N_2 flow rate. The initial concentrations of O_2 and SO_2 were varied from 8% to 14% by varying the inlet flow rate. Increasing the air flow rate also increased the flow rate of inert N_2.

The position of equilibrium changes when the species concentrations present in the gas mixture changes[2]. According to Le Chatelier's principle, the position of equilibrium moves in such a way as to undo the change that has been made. The equilibrium SO_2 conversion is seen to increase slightly with increasing SO_2 and O_2 mole fraction in the feed gas. Indeed, a high concentration of reactants favours the forward reaction.

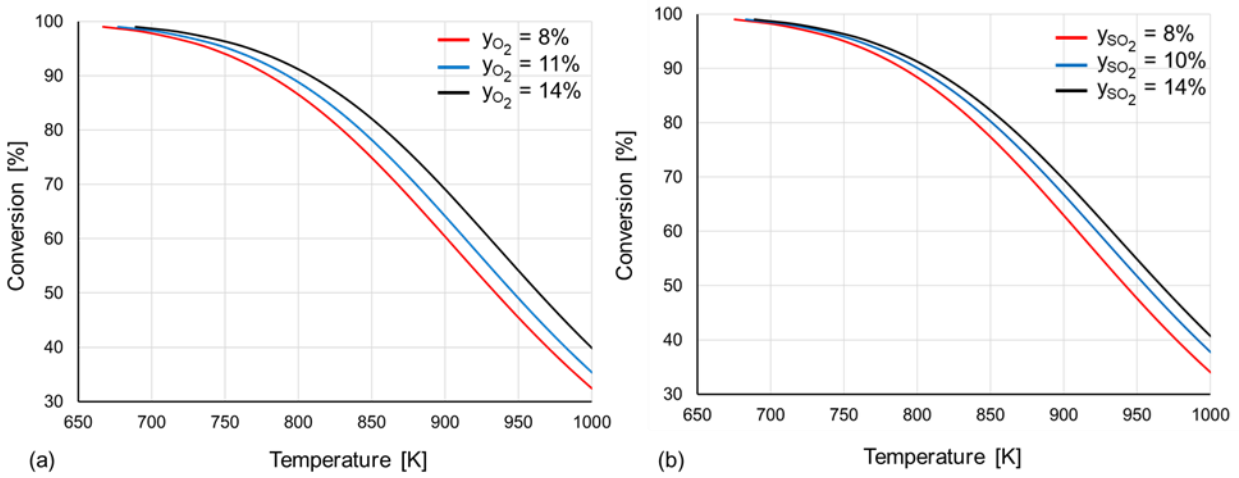

Figure 2-4 Equilibrium curves for constant atmospheric pressure for (a) the effect of O_2 feed concentration on the equilibrium curve, and (b) effect of SO_2 feed concentration on the equilibrium SO_2 oxidation.

2.4 Maximum rate curve

Figure 2-5 presents a series of constant reaction rate curves on a conversion-temperature plot for a 10 mol% SO_2, 11 mol% O_2, and 79 mol% N_2 feed gas composition and 1.4 atm total pressure. The shape of the initial portion of a constant rate curve is due the combination of the increase in the reaction rate with temperature and the decrease of the reaction rate with conversion. As the constant rate curve moves toward the equilibrium curve, it goes to a maximum point corresponding the maximum rate of reaction for a given combination of conversion and temperature. Each constant rate curve is subjected to the same fate. For higher constant reaction rates, the maximum occurs at lower conversion and higher temperature. If it would be possible to adjust the temperature of the packed bed reactor as a function of conversion to constantly follow the maximum rate curve, it

would require a length of bed or catalyst weight that would be minimum for a given conversion. This would be an ideal packed reactor. It is therefore interesting to determine this minimum bed length to offer a comparison with different adiabatic process strategies. The maximum reaction rate curve is determined as a function of conversion and temperature using Eq. (20). For a given conversion, the temperature is changed until the maximum rate is obtained.

$$\frac{\partial r_{SO_2}(X,T)}{\partial T} = 0 \tag{20}$$

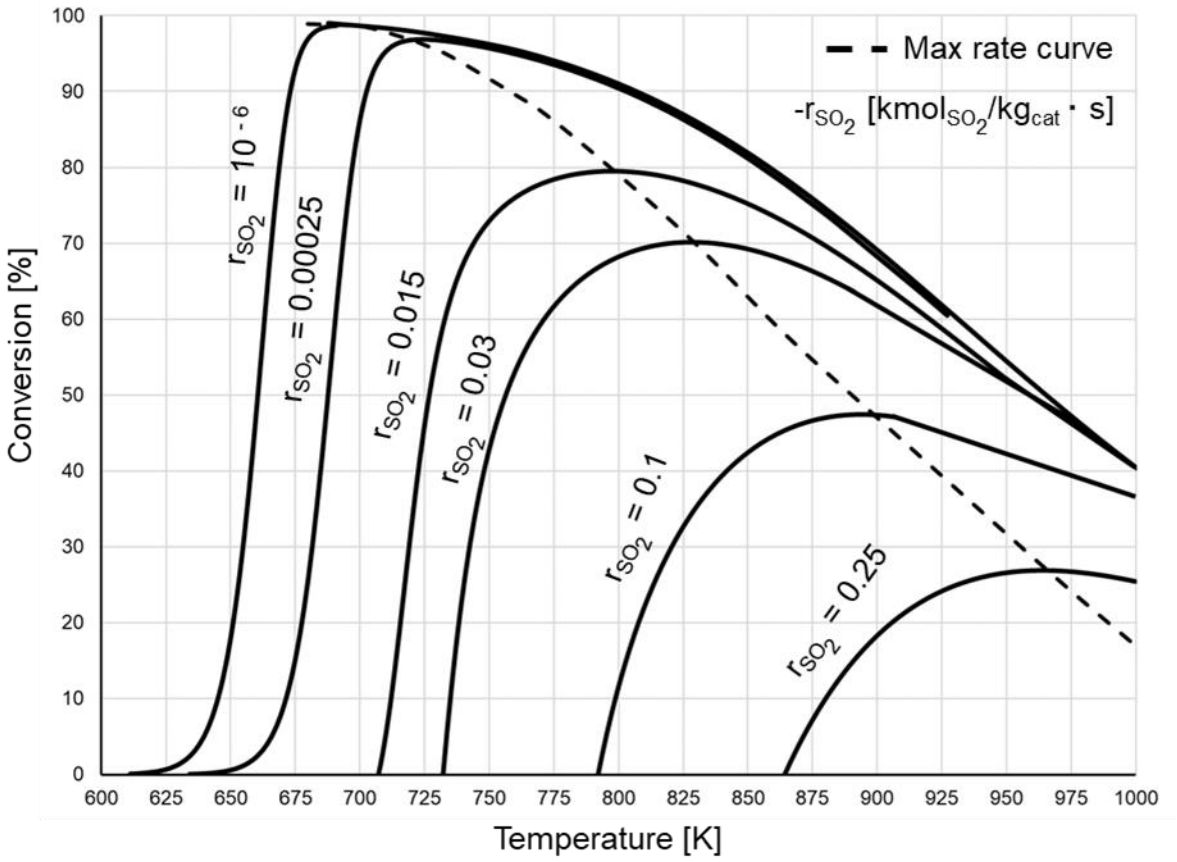

Figure 2-5 Maximum reaction rate curve for the SO_2 oxidation for a 10 mol% SO_2, 11 mol% O_2, and 79 mol% N_2 feed gas composition and 1.4 atm.

2.5 Results and discussion

The aim of this investigation was to identify the kinetic model that best represents the experimental data, which has been tabulated in Appendix A, for the SO_2 oxidation to SO_3. The four different SO_2 oxidation kinetic models presented in Section 2, namely Collina et al.[18], Eklund[15], Calderbank[14] and Villadsen et al.[17], were assessed for their ability to predict the experimental data[13] under different operating conditions. The residual sum of squares (RSS) of the differences between the predicted and experimental data was calculated for each kinetic model to evaluate which kinetic model appears to be more reliable to represent the experimental data in the range of temperature pertaining to the industrial SO_2 reactor.

2.5.1 Experimental versus predicted reaction rate

Kinetic data for the sulphur dioxide oxidation, obtained from an experimental design conducted by Doering et al.[13] was used in this investigation to assess the ability of each kinetic model to represent the experimental data. In the experimental design of Doering et al.[13], four to six conversion data between 90% and equilibrium curve were used to measure the rate of reaction for each gas feed composition, pressure and temperature. A total of 135 experimental data points were available. In this study, this set of experimental data was the basis of comparison to select a proper kinetic rate equation.

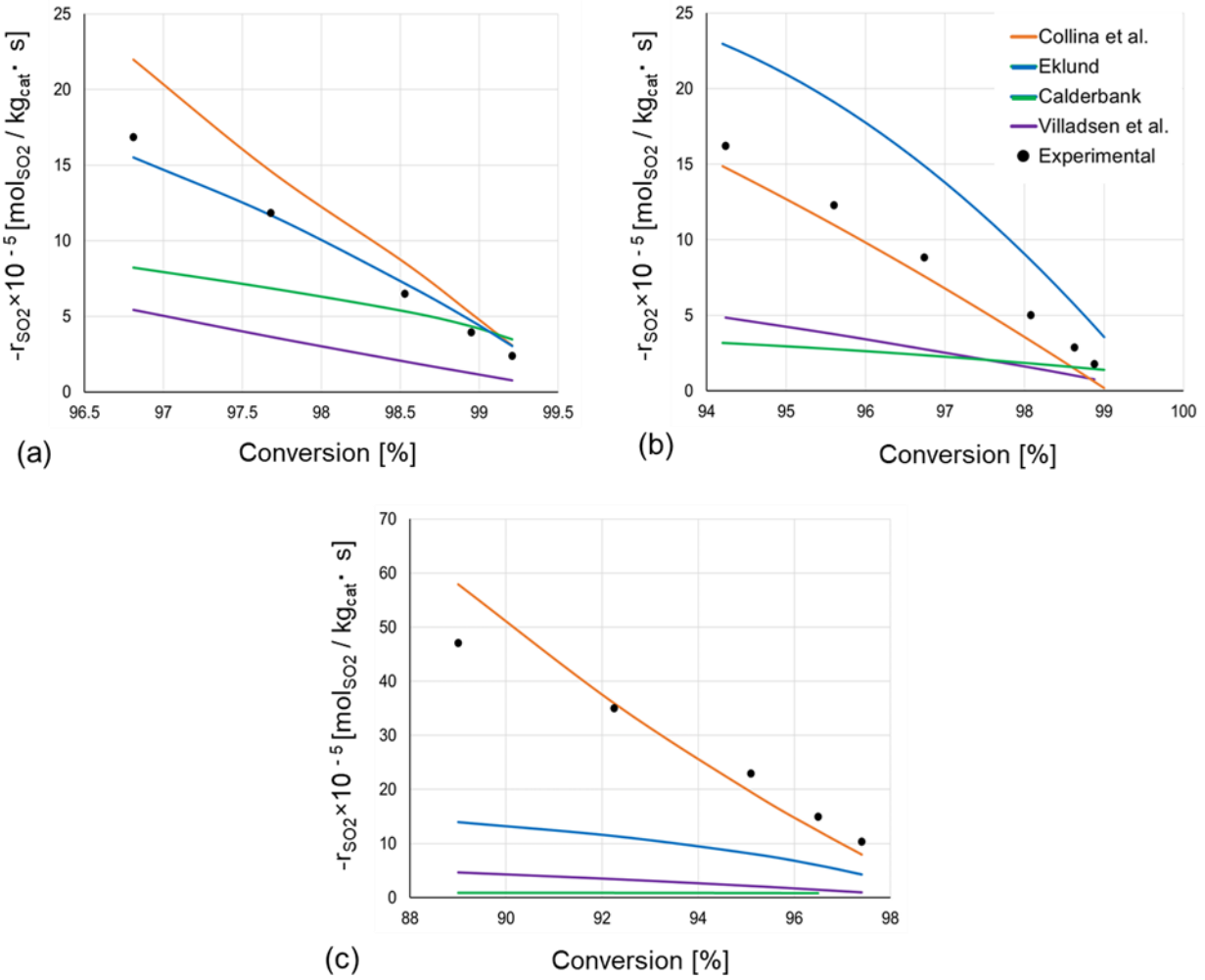

Figure 2-6 Comparison of the experimental and predicted reaction rate as a function of conversion at T = 400˚C: (a) 11 mol% SO_2, 10 mol% O_2 and P = 10 atm; (b) 11 mol% SO_2, 10 mol% O_2 and P = 2.5 atm; (c) 10 mol% SO_2, 11 mol% O_2 and P = 1.12 atm

The comparison of the data at 400˚C and for a feed composition of 11 mol% SO_2, 10 mol% O_2 and a pressure of 10 and 2.5 atm as well for a gas feed composition of 10 mol% SO_2, 11 mol% O_2 and 1.12 atm are presented in Figure 2-6 Two important observations can be made from the results of Figure 2-6. The Eklund kinetic model better represents the experimental data at a pressure near 10 atm (Figure 2-6a). However, the Collina et al. kinetic model predicts with a relatively good accuracy the experimental data at the two lower pressures, including near atmospheric pressure. Similar results were obtained at other experimental conditions. One can conclude that there is no unique

reaction kinetic model that represents the kinetic data over the entire range of the experimental.

2.5.2 Data treatment and results analysis

To better compare the different reaction kinetic models for the complete experimental data set in the databank, the residual sum of squares of the differences between the predicted and experimental data was calculated (Eq. (21)) and used to assess the predictive performance of each kinetic model.

$$\mathrm{RSS} = \sum_{i=1}^{N} \left(\frac{r_{e,SO_{2i}} - r_{SO_{2i}}}{r_{e,SO_{2i}}}\right)^2 \tag{21}$$

where $r_{e,SO_{2i}}$ is the experimental rate of i-th experimental point, $r_{SO_{2i}}$ is the calculated rate of the i-th experimental point according to the reaction mechanism model, and N is the of experimental points considered.

The residual sum squares of each kinetic model for different operating conditions are presented in Figure 2-7. Figure 2-7(a) shows the RSS for different temperatures at a constant pressure of 2.5 atm and feed gas composition (10 mol% SO_2, 11 mol% O_2). When the temperature is increased, the RSS decreases significantly for all kinetic models, which indicates that the models are more accurate if the reaction occurs above 400˚C. The models of Collina et al. and Eklund have the lowest RSS values compared to other models.

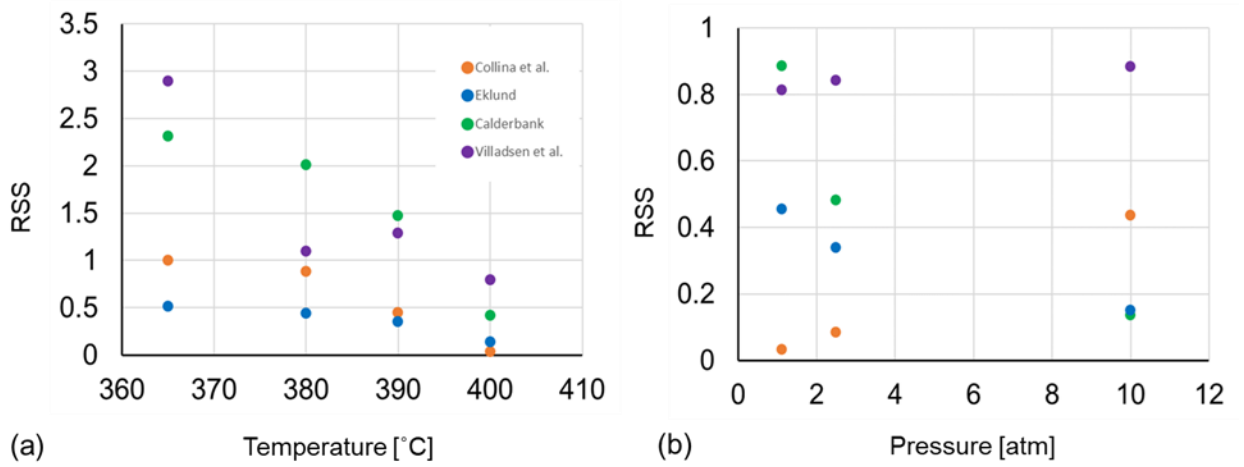

Figure 2-7 Residual sum squares (RSS) of each kinetic model for feed gas compositions of 10 mol% SO_2, 11 mol% O_2 for (a) for different temperatures at a constant pressure of 2.5 atm, and (b) different pressures at the constant temperature (400˚C).

Figure 2-7(b) shows the performance of the four kinetic models when the reaction is conducted at different pressures. The model proposed by Collina et al. has the lowest RSS values at a low operating pressures. When the pressure increase, the RSS values increase. In contrast, the models of Eklund and Calderbank show better predictions at higher pressures. No models exist that can used for all experimental conditions. For instance, the model of Collina et al. better represents the experimental data in a pressure range of 1 to 4 atm. By considering the whole experimental pressure range (1 to 10 atm) and the temperature range investigated, the Collina et al. kinetic model has a lower average RSS value and, in general, shows a better fit considering all the experimental data in comparison with other kinetic models (Table 2-2).

A total of 135 experimental data points were used for different temperatures, pressures and gas compositions, which can be included in the RSS function to find the best equation that represents the entire experimental results. Table 2-2 gives the average RSS value of each kinetic model.

Table 2-2 Residual sum of squares for different kinetic models over the entire range of the experimental data.

Model equation	**Residual sum of squares (RSS)**
Model 1: Collina et al.[18]	0.756
Model 2: Eklund[15]	0.936
Model 3: Calderbank[14]	3.55
Model 4: Villadsen et al.[13]	2.08

The kinetic model proposed by Collina et al. has the lowest average RSS value (0.756). Using this criterion, this model better represents the entire experimental data than the other models. To perform a multi-objective optimization (MOO) for SO_2 oxidation to SO_3 in the plug flow reactor, it is recommended to use the model of Collina et al., especially for pressure near atmospheric and for the feed gas composition of 10 mol% SO_2, 11 mol% O_2.

Conclusions

This work presented the evaluation of four kinetic models for the SO_2 oxidation to SO_3 using vanadium pentoxide catalysts. The oxidation of SO_2 to SO_3 is an equilibrium reaction and the oxidation efficiency increased with increasing the concentration of sulphur dioxide and oxygen in the feed gas. Moreover, in the higher pressures, the equilibrium conversion will be enhanced.

By considering the residual sum of squares to compare different kinetic models using a set of experimental data, it was found that the applicability of the models depends on the operating conditions. A kinetic equation has been selected among the proposed ones to explain experimental data in a narrow range of reaction conditions. Even though the four kinetic models propose different reaction mechanisms and were obtained under different operating conditions, the information obtained in this investigation is still very useful as a guide to decide an experimental plan to obtain the kinetics of the proposed

system. In this investigation, the Collina et al. kinetic model was chosen because it was more comprehensive and detailed as it covers a wide range of reaction conditions.

The determination of the residual sum of squares of all kinetic models allowed to evaluate the range of validity of the operating conditions for a specific kinetic model and to guide in the selection of an appropriate kinetic model. Results showed that the equation was proposed by Collina et al. best represents the experimental results in the range of operating conditions. Finally, this model could be selected to conduct a multi-objective optimization for the catalytic oxidation reactor of the sulphur dioxide to the sulphur trioxide in the plug flow reactor (PFR) for 10 mol% SO_2, 11 mol% O_2 and at the pressure near atmospheric due to the lowest error under this operating conditions and to ensure the expected optimal region within the real domain is enclosed.

Acknowledgments

The authors gratefully acknowledge the financial support for this project provided by the Natural Science and Engineering Research Council of Canada.

Abbreviations

MOO	Multi-objective optimization
PFR	Plug flow reactor
RSS	Residual sum square

Nomenclature

k_1	Rate coefficient for a catalytic reaction [Table 2-1]
k_2	Rate coefficient for a catalytic reaction [$kmol/kg_{cat} \cdot atm \cdot s$]
K_i	Equilibrium coefficient [Table 2-1]
K_P	Equilibrium constant [$atm^{-0.5}$]
P_i	Partial pressure [atm]
P_t	Total pressure [atm]
r_{e,SO_2}	The experimental rate for the SO_2 oxidation [$mol_{SO2}/kg_{cat} \cdot s$]

r_{SO_2}	Reaction rate for the SO_2 oxidation [$mol_{SO2}/kg_{cat} \cdot s$]
T	Temperature [K]
X	Conversion [%]
y_i	Mole fraction of feed gas compositions [%]

Appendices

Appendix A- Experimental results

Table 2-3A Literature experimental data[13]

Operating conditions						Experimental results
T[˚C]	T[K]	P[atm]	%SO_2	%O_2	%X	$R_{SO2}\times10^5$ [$mol_{SO2}/kg_{cat}\cdot s$]
403.4	676.55	10	10.92	10.02	99.21	2.083
403.6	676.75	10	10.93	10.06	98.95	3.435
403.7	676.85	10	10.9	10.01	98.53	5.658
403.5	676.65	10	10.97	10.04	97.68	10.32
403.6	676.75	10	11.02	10.05	96.81	14.69
395	668.15	2.5	10.92	10.02	98.51	1.844
395	668.15	2.5	10.91	10.05	98.32	2.936
394.4	667.55	2.5	11.01	10.08	97.19	5.171
365.5	638.65	10	10.86	10.11	99.67	0.205
365.8	638.95	10	10.93	10.06	99.66	0.406
365.3	638.45	10	11.15	10.12	99.52	0.834
365.6	638.75	10	10.92	10.12	99.05	1.519
365.4	638.55	10	11.14	10.04	97.74	3.593
369	642.15	2.5	10.83	10.05	99.14	0.209
369.3	642.45	2.5	10.78	10.03	99.26	0.44
369.8	642.95	2.5	10.83	10.05	98.32	0.798
395	668.15	10	13.08	14.07	99.7	0.737
395.6	668.75	10	12.78	14.09	99.48	1.421
395	668.15	10	13.24	14.05	99.34	2.548
394.3	667.45	10	13.23	14.06	98.74	5.166
394.6	667.75	2.5	13.35	14.03	99.06	1.299
393.7	666.85	2.5	13.18	14.03	98.84	2.213
396	669.15	2.5	12.9	13.94	98.67	2.444
395	668.15	2.5	13.34	13.94	97.89	5.123
395.4	668.55	2.5	13.21	13.92	96.93	7.716
396.7	669.85	2.5	13.58	13.83	96.12	9.556
377.5	650.65	5	13.01	14.23	99.7	0.12
378.1	651.25	5	12.76	14.29	99.67	0.414

378.9	652.05	5	13.04	14.28	99.61	0.775
378.6	651.75	5	12.86	14.31	99.32	1.846
379.3	652.45	5	12.71	14.3	99.04	2.637
378.5	651.65	5	12.93	14.1	98.5	3.649
361.7	634.85	10	12.99	14.31	99.86	0.033
362.4	635.55	10	12.98	14.31	99.87	0.054
362.9	636.05	10	12.9	14.36	99.86	0.135
362.7	635.85	10	12.99	14.31	99.71	0.74
362.3	635.45	10	12.93	14.3	99.59	1.164
363.4	636.55	10	13.25	14.26	99.41	1.696
364.1	637.25	2.5	13.16	14.14	99.75	0.072
364.6	637.75	2.5	13.36	13.99	99.75	0.113
365	638.15	2.5	13.51	13.52	99.68	0.205
365.3	638.45	2.5	12.72	13.25	99.39	0.74
364.6	637.75	2.5	12.48	13.39	98.99	1.24
365.5	638.65	2.5	12.04	13.62	98.59	1.545
391.6	664.75	10	9.08	14.14	99.51	1.404
390.8	663.95	10	9.08	14.13	99.42	2.251
390.6	663.75	10	9.06	14.15	99.18	3.922
390.8	663.95	10	9.13	14.19	98.55	7.414
391.6	664.75	10	9.14	14.08	97.98	10.44
392.2	665.35	10	9.43	14.01	97.12	14.3
376.6	649.75	5	8.78	14.16	99.84	0.048
376.7	649.85	5	8.94	14.23	99.72	0.223
377.1	650.25	5	8.85	14.22	99.64	0.537
376.6	649.75	5	8.96	14.19	99.42	1.252
377	650.15	5	8.87	14.24	99.19	1.94
378.9	652.05	5	9.31	14.1	98.93	2.594
364.3	637.45	10	9.37	14.24	99.63	0.064
364.4	637.55	10	9.58	14.21	99.61	0.22
364.6	637.75	10	9.54	14.23	99.55	0.561
364.3	637.45	10	9.64	14.21	99.35	1.305
363.9	637.05	10	9.68	14.26	99.12	1.924
363.9	637.05	10	9.91	14.16	98.89	2.614
364.5	637.65	2.5	9.02	14.13	99.57	0.109
364.8	637.95	2.5	9.02	14.08	99.47	0.275
365.7	638.85	2.5	8.95	13.7	99.31	0.583
365.5	638.65	2.5	8.92	13.74	98.89	1.204
366.6	639.75	2.5	8.81	13.78	98.51	1.769
366.9	640.05	2.5	9.25	13.88	97.97	2.549
395.3	668.45	2.5	9.16	14.15	98.88	1.541
395.6	668.75	2.5	8.99	14.07	98.63	2.504
395.4	668.55	2.5	9.42	14.05	98.08	4.37
392.5	665.65	2.5	9.17	14.24	96.74	7.688

393	666.15	2.5	9.18	14.21	95.6	10.69
392.7	665.85	2.5	9.41	14.25	94.24	14.1
392.6	665.75	10	8.87	8	99.4	0.588
392.7	665.85	10	8.81	8.02	99.27	0.883
393.1	666.25	10	8.86	7.95	99.21	1.12
393	666.15	10	8.86	7.91	98.86	2.67
393.2	666.35	10	8.85	7.9	98.5	4.025
393	666.15	10	9.14	7.89	98.12	5.469
394.3	667.45	2.5	8.52	7.98	98.92	0.5
394.9	668.05	2.5	8.47	7.91	98.74	0.935
395	668.15	2.5	8.64	7.88	98.57	1.401
393	666.15	2.5	8.4	7.97	97.99	2.657
394	667.15	2.5	8.48	7.97	97.4	3.972
394	667.15	2.5	8.73	7.99	96.6	5.017
379	652.15	5	8.48	8.01	99.47	0.133
379.5	652.65	5	8.54	7.84	99.36	0.285
379.5	652.65	5	8.42	7.89	99.23	0.599
380.2	653.35	5	8.41	7.9	98.95	1.269
380	653.15	5	8.53	7.84	98.64	1.012
379.6	652.75	5	8.74	7.86	98.24	2.531
365	638.15	10	8.52	7.96	99.57	0.103
363.5	636.65	10	8.43	7.87	99.51	0.55
363.7	636.85	10	8.49	7.86	99	1.215
363.5	636.65	10	8.5	7.83	98.59	1.813
363.5	636.65	10	8.58	7.79	97.92	2.245
364.7	637.85	2.5	8.14	8.22	99.56	0.156
364.7	637.85	2.5	8.3	8.05	99.35	0.312
365.4	638.55	2.5	8.21	8.14	99.02	0.603
380	653.15	10	11	10	97.58	5.7
380	653.15	10	11	10	98.55	3.9
380	653.15	10	11	10	99.37	2.1
380	653.15	10	11	10	99.67	1.2
380	653.15	10	11	10	99.8	0.67

References

1. Kiss, A., S.Bildea, C. & Grievink, J. Dynamic modeling and process optimization of an industrial sulfuric acid plant. Chem. Eng. J. 158, pp 241–249 (2010).
2. King, M. J., Davenport, W. G. & Moats, M. S. Overview. in Sulfuric Acid Manufacture Elsevier, pp 1–9 (2013).
3. Doering, F. J. & Berkel, D. A. Comparison of kinetic data for K V and Cs V sulfuric acid catalysts. J. Catal. 103, pp 126–139 (1987).

4. Tandy, G. H. The role of alkali sulphates in vanadium catalysts for sulphur dioxide oxidation. J. Appl. Chem.6 , pp 68–74 (2007).

5. Harris, J. L. & Norman, J. R. Temperature-Dependent Kinetic Equation for Catalytic Oxidation of Sulfur Dioxide. Ind. Eng. Chem. Process Des. Dev. 11, pp 564–573 (1972).

6. Shi, Y. & Fan, M. Reaction kinetics for the catalytic oxidation of sulfur dioxide with microscale and nanoscale iron oxides. Ind. Eng. Chem. Res. 46, pp 80–86 (2007).

7. Colom, J. M. et al. Importance of Vanadium-Catalyzed Oxidation of SO_2 to SO_3 in Two-Stroke Marine Diesel Engines. Energy and Fuels 30, pp 6098–6102 (2016).

8. Yeramian, A. A., Silveston, P. L. & Hudgins, R. R. Influence of inert gases on the catalytic oxidation of SO_2. Can. J. Chem. 36, pp 496–506 (1958).

9. Mars, P. & Maessen, J. G. H.The mechanism and the kinetics of sulfur dioxide oxidation on catalysts containing vanadium and alkali oxides. J. Catal.10, pp 1–12 (1968).

10. King, M. J., Davenport, W. G. & Moats, M. S. Materials of construction. in Sulfuric Acid Manufacture Elsevier, pp 349–356 (2013).

11. Clark, D., Vavere, A. & R. Horne, J. Using Super Cesium Catalyst to Increase Sulfuric Acid Production. AIChE Conv. Clear. pp 1–6 (2007).

12. Belo, L. P. et al. High-temperature conversion of SO_2 to SO_3: homogeneous experiments and catalytic effect of fly ash from air and oxy0fuel firing. Energy and Fuels 28, pp 7243–7251 (2014).

13. Doering, F. J., Unland, M. L. & Berkel, D. A. Modelling of SO_2 oxidation rates based on kinetic data of a Cs/V catalyst at high pressures and conversions. Chem. Eng. Sci. 45, pp 1939–1941 (1988).

14. Calderbank P H. The mechanism of the catalytic oxidation of sulphur dioxide with a commercial vanadium catalyst: A kinetic study. J. App. Chem.; pp 482-492.(1952)

15. Eklund R. B., Dissertation in the Manufacture of Sulfuric, Royal Institute of Technology, Stockholm, pp. 166–168. (1956)

16. Doering, F. J. & Gaddy, J. L. Optimization of the sulfuric acid process with a flowsheet simulator. Comput. Chem. Eng. 4, pp 113–122 (1980).

17. Villadsen, J. & Livbjerg, H. Kinetics and effectiveness factor for SO2 oxidation on an industrial vanadium catalyst. Chem. Eng. Sci. 27, pp 21–38 (1972).

18. Collina, A., Corbetta, D., and Cappelli, A., "Use of Computers in the Design of Chemical Plants", in Proc. Eur. Symp, Firenze, pp 329 (1971).

Chapter 3. Modelling and multi-objective optimization of the sulphur dioxide oxidation process

Mohammad Reza Zaker, Jules Thibault, Clémence Fauteux-Lefebvre
Department of Chemical and Biological Engineering
University of Ottawa
Ottawa, Ontario, Canada K1N 6N5

Abstract

Sulphuric acid (H_2SO_4) is one of the most commonly produced chemicals in the world, which is widely used in a range of industrial processes and manufacturing. The critical step of the sulphuric acid production is the catalytic oxidation of sulphur dioxide (SO_2) to sulphur trioxide (SO_3) which takes place in a heterogeneous plug flow catalytic reactor. This study presents the multi-objective optimization of the SO_2 oxidation for various scenarios involving a number of catalytic beds and different reactor configurations. In the optimization process, a number of input or decision variables are used to determine the optimal values of the three targeted objective criteria: SO_2 conversion, SO_3 productivity and catalyst weight. The optimization process is typically comprised of two steps: (1) the Pareto domain is circumscribed by generating a large number of non-dominated solutions via the Non-Dominated Sorting Genetic Algorithm II (NSGA-II), and (2) the Pareto-optimal solutions are ranked based on the preferences of a decision maker. Results show that the strategy where an intermediate SO_3 absorption column is used in the process involving four catalytic beds provides higher SO_2 conversion in the comparison with the same process without an intermediate absorption column. However, the enhanced conversion is achieved at the expense of higher operating costs. The optimum value of the total bed length for the four catalytic beds without an intermediate SO_3 absorption column commonly used industrially, is very closed to its minimum or ideal (5% difference), which clearly shows that the minimum

catalyst weight almost prevails in this strategy to reach a relatively high SO_2 conversion in the vicinity of 97%.

3.1 Introduction

Sulphuric acid is a chemical of paramount industrial importance, where it is used in a myriads of products. Sulphuric acid (H_2SO_4) is a strong mineral acid. It is a colourless and viscous liquid that is soluble in water at all concentrations[1]. Sulphuric acid is a very important commodity chemical and a nation's sulphuric acid production is one of the indicators of its industrial strength[2]. To minimize the risk associated with its transportation, sulphuric acid production plants are usually located near their point of use because sulphuric acid is a corrosive and dangerous acid. In addition, it is more economical and safer to transport elemental sulphur than sulphuric acid[2]. Sulphuric acid is an essential chemical for numerous process industries, such as fertilizer manufacturing, oil refining, chemical synthesis and lead-acid batteries[3].

Originally, sulphuric acid was produced using the "Chamber" process where the oxidation of sulphur dioxide (SO_2) with moist air was oxidized using nitrogen oxides as catalysts. The reaction took place in a series of large, boxlike chambers of lead sheets[2]. Due to the small plant size and product acid strength limited to 70% sulphuric acid, it has been largely supplanted in modern industrial processes by the "Contact process"[4]. The simplified flowsheet of the current industrial sulphuric acid production is shown in Figure 3-1. The sulphuric acid manufacturing is mainly comprised of three steps. In the first step, elemental sulphur is burned in a furnace in the presence of dry air to produce sulphur dioxide. In the second step, sulphur dioxide is oxidized to sulphur trioxide (SO_3) in an adiabatic packed bed reactor using vanadium pentoxide catalyst. This reaction is reversible and highly exothermic. In the final step, an absorption column of concentrated sulphuric acid is used where SO_3 reacts with water to form sulfuric acid. Most plants and smaller units of sulphuric acid plants use a single final absorption process, which leads to a conversion of 96-98%. Some modern large-capacity sulphuric acid production plants utilize a double contact absorption process. By adding an intermediate absorption column, the double contact process can achieve a conversion in excess of 99% but at the expense of a more complex process[2].

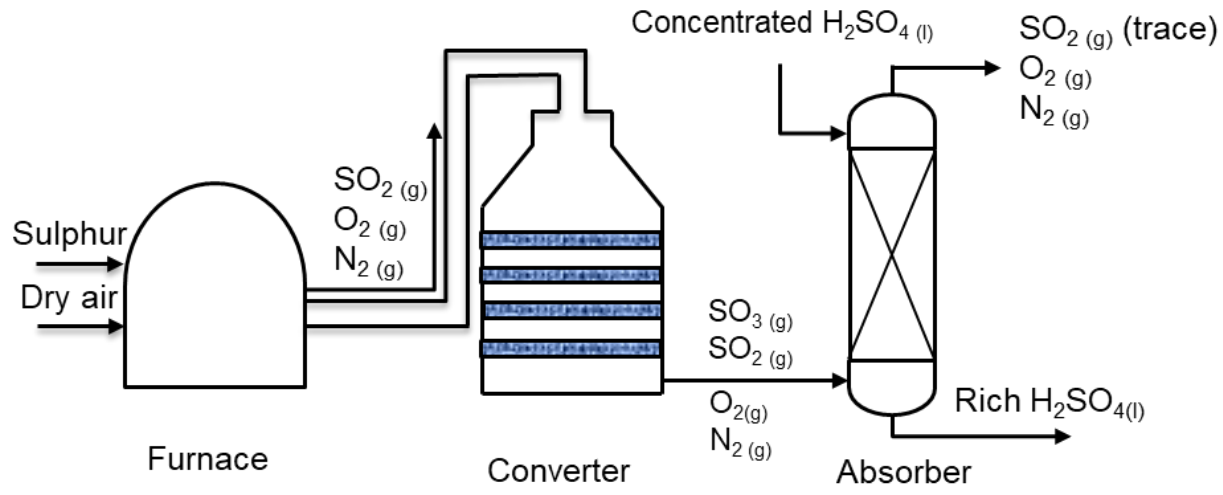

Figure 3-1 Simplified sulphuric acid production flowsheet showing the main three steps: (1) combustion of sulfur to produce SO_2 in presence of dry air, (2) oxidation of SO_2 to SO_3 in a series of adiabatic catalytic packed beds, (3) absorption of sulphur trioxide in a concentrated sulphuric acid absorber and conversion to sulphuric acid.

The critical step in the production of sulphuric acid is the oxidation of sulphur dioxide to sulphur trioxide. Because this reaction is a highly exothermic equilibrium reaction, it takes place in a number of adiabatic catalytic beds with external intercoolers to decrease the temperature prior to entering the next catalytic bed in order to increase the SO_2 oxidation rate. This catalytic reaction initially used platinum as the catalyst. However, the cost of platinum and its susceptibility to poisoning by trace elements led to the development of the vanadium pentoxide catalyst, which is currently used industrially[5].

The typical progression of the SO_2 conversion and the bed temperature for this exothermic equilibrium reaction in a four-bed adiabatic catalytic plug flow reactor is presented in Figure 3-2. The location of the equilibrium curve in Figure 3-2 depends on the inlet composition and pressure of the reacting mixture. The slope of the adiabatic operating lines is a function of the thermal capacity of the reacting mixture and the heat of reaction[6]. The horizontal operating lines represent the cooling of the reaction mixture which takes place between two sequential beds in external heat exchangers[7]. The curve of the maximum rate is the locus of the conversion-temperature coordinates at which the reaction rate is maximum[7].

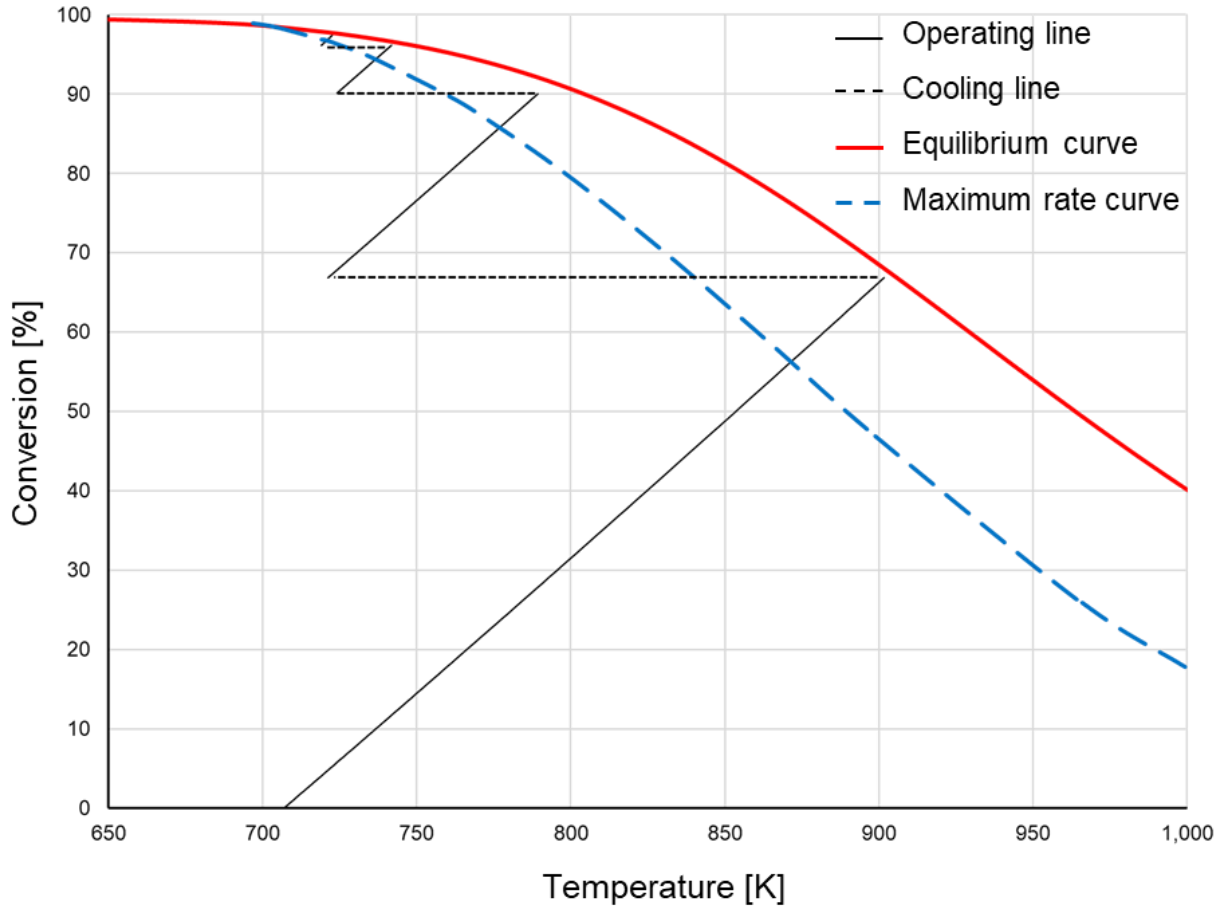

Figure 3-2 Typical conversion versus temperature diagram for the case where four catalytic beds are used to conduct the SO_2 to SO_3 reaction with gas cooling between beds. The equilibrium and maximum rate curves are also drawn.

Given the complexity of the SO_2 to SO_3 reactor configuration, it is paramount to adopt the optimal configuration and to operate the process under optimal conditions. It is obviously desired to maximize the SO_2 conversion, as unreacted SO_2 will need to be treated at the exit of the SO_3 absorption column. However, a high conversion rate can only be achieved at the expense of a low productivity and a large reactor volume, leading to a set of competitive objectives since productivity needs to be maximized whereas the reactor volume needs to be minimized. The optimization of the SO_2 to SO_3 multi-bed reactor is therefore a multi-objective optimization problem where a compromise between the various objectives must be struck. Associated with the best compromised solution is

the set of input or decision variables that has given rise to this optimal solution. In the case of the SO_2 to SO_3 multi-bed catalytic reactor, the decision variables could be the inlet temperature and the length of each catalytic bed, the reactor pressure and the configuration of the packed catalytic beds.

To determine this compromised optimal solution, one can resort to multi-objective optimization (MOO) algorithms that have seen rapid development and application in chemical engineering in recent years. MOO refers to the optimization of multiple and often conflicting objectives, which produces a set of alternative solutions, called the Pareto domain. These solutions, obtained without any bias as to the importance of each objective, are said to be Pareto-optimal in the sense that no one solution is better than any other in the domain when compared on all objectives[8]. The experience and knowledge of the decision-maker are then used to rank the entire Pareto domain.

This investigation is dedicated to the multi-objective optimization of the SO_2 to SO_3 multi-bed catalytic reactor. The first step in the optimization process is to obtain a representative dynamic model of the industrial catalytic bed and most importantly the rate equation, which will be presented in Sections 2 and 3. Secondly, in Section 4, the process model is transformed into a multi-objective problem where decision variables and objectives are defined and used to circumscribe and rank the Pareto domain for numerous process strategies. In Section 5, the performance of the various process strategies in terms of the set of objective functions are presented and discussed.

3.2 Process description

The Contact Process is the current method for the production of sulphuric acid at the concentration levels needed for industrial processes. The contact process was patented in 1901 by Badische Anilin & Soda-Fabric (BASF)[4]. Friedman[4] described the pioneering activities of BASF in the development of the contact process and the selection of a catalyst to promote the oxidation of SO_2 to SO_3. As expected, the catalyst used in the Contact Process only contributes to increase the rate of reaction and does not modify the location of the thermodynamic equilibrium[9].

As explained previously, the sulphuric acid manufacturing consists mainly of three steps: (1) the combustion of elemental sulphur with excess dry air to produce a sulphur

dioxide gas stream, (2) the conversion of SO_2 to SO_3 in a multi-bed catalytic reactor, and (3) the absorption of SO_3 in a highly concentrated sulphuric acid solution where SO_3 reacts with water to form additional sulphuric acid. The chemical reactions associated with the three main steps are given in Eqs. (22)-(24) along with their respective heat of reaction[3]. It is important to note that the three reactions are highly exothermic, and the second reaction is an equilibrium reaction.

$$S_{(s)} + O_{2\,(g)} \rightarrow SO_{2\,(g)} \qquad \Delta H_R = -296810\ [kJ/kmol] \tag{22}$$

$$SO_{2\,(g)} + 0.5\ O_{2\,(g)} \leftrightarrow SO_{3\,(g)} \qquad \Delta H_R = -96232\ [kJ/kmol] \tag{23}$$

$$SO_{3\,(g)} + H_2O_{(l)} \rightarrow H_2SO_{4\,(l)} \qquad \Delta H_R = -132000\ [kJ/kmol] \tag{24}$$

Given the equilibrium exothermic oxidation of SO_2 to SO_3 and based on Le Chatelier's principle, using a lower temperature and higher pressure would favour the forward reaction and would achieve a higher conversion. However, the conventional vanadium pentoxide catalyst has a minimum temperature of approximately 400°C, referred to as the strike temperature, which is the minimum temperature required to initiate a self-sustaining reaction. This minimum temperature is a severe limitation as it limits the range of conversion before equilibrium is reached. Active research is currently under way to find a better catalyst or a promotor to reduce the strike temperature, such as using cesium-promoted vanadium catalyst which is able to lower the initial temperature by 20°C to 40°C. In addition, a higher temperature leads to a higher rate of reaction such that process design considerations suggest, as it is done in practice in a sulphuric acid plant, the use of a multi-bed reactor with heat exchangers between the catalytic beds. It is this process that is the subject of the optimization study performed in this investigation.

3.3 Reaction kinetics

Over many decades, several kinetic models for the SO_2 to SO_3 oxidation on the vanadium pentoxide catalyst have been proposed (Collina et al.[10], Eklund[11], Calderbank[12], Villadsen et al.[13]). In this investigation, the kinetic model suggested by Collina et al.[10] was used for the purpose of the multi-objective optimization (MOO). This

kinetic model was retained because it better represents the experimental data available in the temperature range of interest than the other kinetic models,

The kinetic model of Collina et al. is based on the Hougen-Watson[10] concept and on the observation that the reaction between adsorbed SO_2 and oxygen from the gas phase is the rate-controlling step. The rate expression of the SO_2 oxidation, presented in Eq. (4) is related to the partial pressures of SO_2, O_2 and SO_3. This rate expression was derived for the specific catalyst that is used industrially.

$$-r_{SO_2} = \frac{k_1 \cdot p_{O_2} \cdot p_{SO_2}\left(1 - \frac{p_{SO_3}}{K_p \cdot p_{SO_2} \cdot p_{O_2}^{0.5}}\right)}{22.414(1 + K_2 \cdot p_{SO_2} + K_3 \cdot p_{SO_3})^2} \qquad \left[\frac{kmol}{kg_{cat} \cdot s}\right] \tag{25}$$

where

$$K_p = \exp\left(-10.68 + \frac{11300}{T}\right) \qquad [atm^{-0.5}] \tag{26}$$

$$k_1 = \exp\left(12.16 - \frac{5473}{T}\right) \qquad \left[\frac{kmol}{kg_{cat} \cdot atm \cdot s}\right] \tag{27}$$

$$K_2 = \exp\left(-9.953 + \frac{8619}{T}\right) \qquad [atm^{-1}] \tag{28}$$

$$K_3 = \exp\left(-71.745 + \frac{52596}{T}\right) \qquad [atm^{-1}] \tag{29}$$

3.4 Reactor modelling

Industrially, the SO_2 to SO_3 oxidation is typically conducted adiabatically in a series of large diameter packed catalytic reactors with inter-reactor heat exchangers. Each packed bed reactor has a height between 0.02 to 2.0 m and a diameter varying between 5 to 12 m. It is assumed that ideal plug flow conditions prevail with negligible axial and radial dispersion such that the integration of the mass and heat transfer equations is performed only in the axial direction. In addition, it is assumed that the reactor operates under steady state. The general molar balance equation describing the SO_2 conversion (X) along the axial direction of reactor bed is given by Eq. (30).

$$\frac{dX}{dz} = \frac{-r_{SO_2} \cdot \rho_b \cdot A}{(F_{SO_2})_{in}} \tag{30}$$

Since the SO_2 oxidation reaction is very exothermic and the reaction rate is strongly dependent on temperature, the steady-state one-dimensional energy balance must also be solved to determine the variation of temperature along the bed as described in Eq. (31). It is assumed that both the axial thermal dispersion and the radial gradient are negligible.

$$\frac{dT}{dz} = \frac{-r_{SO_2} \cdot \rho_b \cdot A \cdot \Delta H_R}{C_{P_{Mix}}} \tag{31}$$

where $C_{p,Mix,}$ and ΔH_R are heat capacity and heat of reaction, respectively. Their temperature dependencies are discussed in Appendices A and B, respectively.

The rate of reaction depends on the partial pressure of the two reactants and the product. To determine the pressure drop through the packed beds, the Ergun equation, giving the change of pressure as a function of the bed length, is used (Eq. (32)).

$$\frac{dP}{dz} = 150 \times \frac{\mu \cdot u \cdot (1-\varepsilon)^2}{D_p^2 \cdot \varepsilon^3} + 1.75 \times \frac{\rho_f \cdot u^2 \cdot (1-\varepsilon)}{D_p \cdot \varepsilon^3} \tag{32}$$

To determine the conversion, temperature and pressure as a function of position along the packed bed, the packed bed is discretized in a number of thin slices. For each slice, the heat of reaction, heat capacity, viscosity, reaction rate coefficients with their respective temperature dependencies are determined, and the operating conditions are therefore set to carry out the calculations for the next slice of the catalytic bed reactor. The mass and energy balance equations, and the Ergun equation are numerically integrated starting with the inlet conditions of the gas mixture till the end of the last catalytic bed. The SO_2 conversion, SO_3 productivity and catalyst weight are then evaluated as described in Eqs. (33)-(35), respectively.

$$\text{Conversion (X)} = \frac{(F_{SO_2})_{in} - (F_{SO_2})_{out}}{(F_{SO_2})_{in}} \times 100 \quad [\%] \tag{33}$$

$$\text{Productivity (Pro)} = \frac{F_{SO_3}}{A \times \rho_b \times \sum L_i} \quad [\frac{mol}{kg_{cat} \cdot s}] \quad (34)$$

$$\text{Catalyst weight (W)} = A \times \rho_b \times \sum L_i \quad [kg] \quad (35)$$

3.4.1 Operating conditions

In this study, the pressure of the inlet gas mixture to the sulphur dioxide converter was set slightly higher than atmospheric pressure, namely at 1.4 atm. A 12-m diameter adiabatic catalytic reactor was selected with a feed gas flow rate of 800 mol/s. The inlet temperature and the length of each catalytic bed are decision variables and will be adjusted with the optimization algorithm in order to determine all Pareto-optimal solutions, each solution being comprised of the conversion, productivity and catalyst weight. All simulation parameters such as the bed porosity, bed bulk density, gas mixture density, etc. are given in Table 3-1.

Table 3-1 Reactor system simulation parameters

Parameter	Description	Value
ε	Bed porosity	0.303
ρ_b	Bed density	256 [kg/m^3]
ρ_f (T=460°C)	Inlet gas density	0.781 [kg/m^3]
A	reactor area	113 [m^2]
D_{bed}	Bed diameter	12 [m]
D_p	Equivalent particle diameter	6.35×10^{-3} [m]
F_{in}	Inlet flow rate	800 [mol/s]
P_{in}	Inlet pressure	1.4 [atm]
R	Gas constant	8.314 [Pa·m^3/mol·K]
$y_{N_2,\,in}$	Inlet mole fraction of SO_2	0.10

$y_{O_2,\ in}$	Inlet mole fraction of O_2	0.11
$y_{SO_2,\ in}$	Inlet mole fraction of N_2	0.79
$y_{SO_3,\ in}$	Inlet mole fraction of SO_3	0.0

3.5 Multi-objective optimization

In this investigation, the oxidation of SO_2 to SO_3 is optimized using a multi-objective optimization approach. The optimization methodology comprises four main steps as illustrated in Figure 3-3. The optimization problem is first established by defining the set of objective functions to be maximized or minimized, and the set of decision variables with their respective allowable ranges. The next step is determining a representative process model to perform the optimization study. In this investigation, the process model is comprised of the integration along the axial direction of the steady-state heat and mass balances and the pressure drop equations (Eqs. (9)-(11)), which allows to determine the three objective functions: conversion (X), productivity (Pro), and catalyst weight (W) (Eq. (12)-(35)). Once the packed-bed catalytic reactor model is available, it is used to circumscribe the Pareto domain using a MOO algorithm. In this investigation, the Non-Sorting Genetic Algorithm II (NSGA II) has been used[14]. Finally, all Pareto-optimal solutions are ranked using the Net Flow Method (NFM) where the preferences of a decision-maker are embedded in a set of relative weights and three threshold criteria to assist in the ranking of all Pareto-optimal solutions.

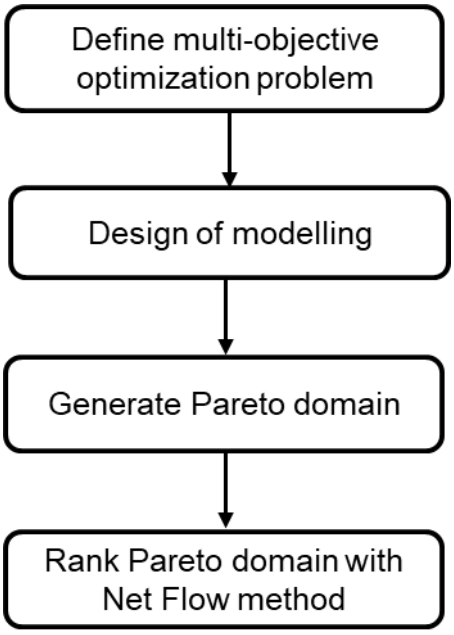

Figure 3-3 Flowchart of the methodology for solving the multi-objective optimization problem.

3.5.1 Definition of the optimization problem

In multi-objective optimization, it is desired to determine the best set of operating conditions (decision variables) that will lead to an ensemble of objective functions that is considered optimal based on the knowledge and expertise of the decision-maker. There is no unique way to define an optimization problem and may involve many iterations before reaching a satisfying problem definition. In this investigation, the ensemble consists of three objective functions that are deemed to have an impact on the efficiency and economics of the process: the SO_2 conversion (X), the SO_3 productivity (Pro) and the catalyst weight (W), as defined in Eqs. (33)-(35). It is desired to maximize the first two objective functions and to minimize the latter one. A summary of the input variables and the objective functions is presented in Table 3-2. A multi-objective optimization problem can be defined mathematically in general terms using Eq. (15) where it is desired to maximize the ensemble of objective functions (**F(x)**) by choosing the set of decision or input variables (**x**) such that to satisfy some equality and inequality constraints. In addition, the values of each input variables must be drawn within their feasible range (see Table 2 for lower and upper bounds). The feasible range of the decision variables was

chosen large enough to ensure that all Pareto optimal solutions were well within that range. In this investigation, various configurations of the catalytic packed bed reactor were evaluated and the number of decision variables varies between two and eight. In this investigation, there were no equality of inequality constraints.

$$\begin{aligned} &\text{Max } \mathbf{F(x)} = (X(\mathbf{x}), Pro(\mathbf{x}), -W(\mathbf{x})) \\ &\quad \text{Subject to} \quad h_j(\mathbf{x}) = 0 \quad j = 1, \cdots, J \\ &\qquad\qquad\quad g_n(\mathbf{x}) \geq 0 \quad n = 1, \cdots, N \\ &\qquad\qquad\quad (x_i)_{min} \leq x_i \leq (x_i)_{max} \quad i = 1, 2, \cdots, 8 \end{aligned} \tag{36}$$

3.5.2 Pareto domain

The Pareto domain is defined as the collection of solutions taken from the total solution set that are non-dominated when compared to the other solutions within this set. A solution is said to be dominated by another solution if the values of all optimization objectives of the first solution are worse than those of the second. Moreover, a non-dominated or Pareto-optimal solution is obtained if no other feasible solution dominates it. Because engineering problems are usually complex, it is not possible to derive an analytical solution to represent the Pareto domain; instead it is represented by a large number of solutions obtained using an iterative procedure. The Pareto front in the objective space represents the optimal trade-off among all objective functions. If the objectives were not conflicting, which is rarely the case, the Pareto domain would contain a unique solution that maximizes or minimizes all objectives. In this investigation, the conversion and the productivity are clearly conflicting.

For the optimization of the SO_2 oxidation to SO_3, many operating strategies were explored. All strategies had the same set of objective functions but with different number of decision variables. The decision variables are the inlet temperature and the length of each catalytic bed. Figure 3-4 presents a schematic diagram of the optimization process when four catalytic beds in series were used such that eight decision variables need to be considered.

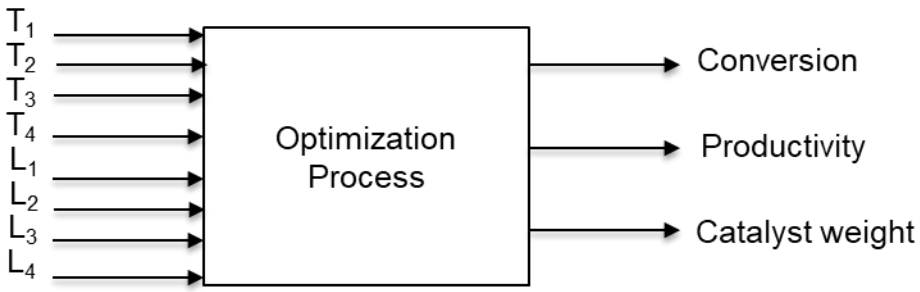

Figure 3-4 Schematic of the optimization of the SO_2 oxidation to SO_3. This optimization problem considered for the scenario where four catalytic beds in series are used. The eight decision variables are the inlet temperature and the length of each catalytic bed.

Table 3-2 Input and output process variables

Variables		
Decision variables	**Identifier**	**Range and units**
Temperature		
First bed	T_1	600-900 [K]
Second bed	T_2	600-900 [K]
Third bed	T_3	600-900 [K]
Fourth bed	T_4	600-900 [K]
Length		
First bed	L_1	0.02-2 [m]
Second bed	L_2	0.02-2 [m]
Third bed	L_3	0.02-2 [m]
Fourth bed	L_4	0.02-2 [m]
Objective functions	**Identifier**	**Desired attributes**
Conversion	X	Maximize
Productivity	Pro	Maximize
Catalyst weight	W	Minimize

3.5.3 Non-sorting genetic algorithm II (NSGA II)

Although, in principle at least, the Pareto domain could be examined from the generation of the entire solution set, in practice this is impractical. Alternatively, diverse algorithms have been developed to have a reasonable representation of the Pareto domain from a limited number of solutions. One such method, referred to as the Non-Dominated Sorting Genetic Algorithm II (NSGA-II)[14], was used here to determine a finite representation of the Pareto domain. The evolutionary algorithm NSGA is a popular non-

domination based genetic algorithm for multi-objective optimization. It is a very effective algorithm but has been generally criticized for its computational complexity, lack of elitism and for choosing the optimal parameter value for sharing parameters. A modified version, NSGA-II was developed, which has a better sorting algorithm, incorporates elitism and no sharing parameter needs to be chosen a priori. The general procedure of the NSGA-II is summarized in Figure 3-5:

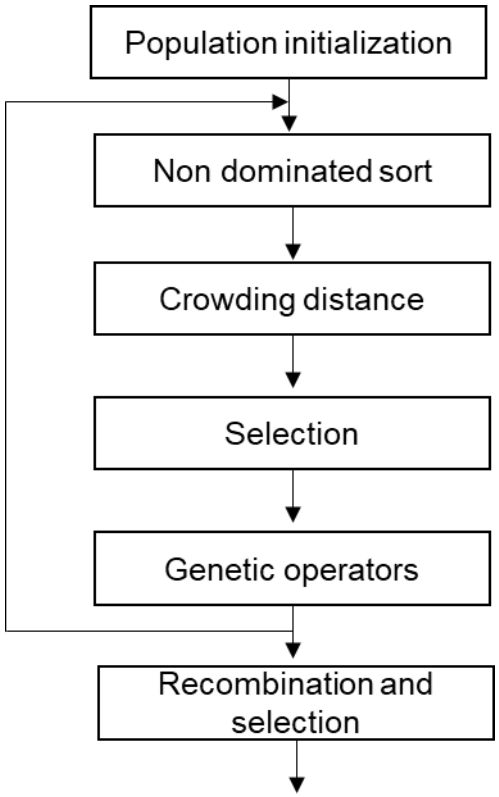

Figure 3-5 Different stages of NSGA-II algorithm are used to adequately circumscribe a large number of representative non-dominated solutions.

The first step in the NSGA-II algorithm consists in generating an initial number of solutions, called the initial population. This is done by randomly selecting values for each of the process inputs or decision variables (inlet temperature and length of each bed) that lie within their lower and upper bounds (see Table 3-2). The model is then solved for all sets of the input variables within the initial population to generate the three objective criteria associated to each set of decision variables. A pairwise comparison is performed of all solutions in the population to determine the number of times a given solution is

dominated, which provides a domination score for each solution. The solutions within the population are then sorted by ascending score of non-domination. The first front is comprised of all solutions with the lowest domination score. The other solutions with higher domination scores are progressively categorized into additional fronts, which indicate their relative performance. A new population of the same size is selected by taking the solutions contained in the fronts with a lower index until the size of the population is exceeded. To make the population equal to the desired size, solutions of the last front are chosen based on the crowding distance to ensure preserving diversity. Parents are selected from the newly created population using binary tournament selection based on the rank and crowding distance. The selected population generates offspring from crossover and mutation operators. The total members of the current population and the current offspring are sorted again based on non-domination and only the best N individuals are selected, where N is the population size[15]. This procedure is followed until the desired number of generations are performed.

3.5.4 Multicriteria optimization algorithm: net flow method (NFM)

When the Pareto domain has been circumscribed, the next step consists of ranking all Pareto-optimal or non-dominated solutions. The Pareto domain has been established through a domination perspective without the bias of a priori knowledge. However, to rank each solution of the Pareto domain, the decision-maker now needs to express his or her preferences based on the knowledge that (s)he has of the process. There are many methods for ranking the Pareto domain. In this investigation, a multi-criteria optimization algorithm, known as the net flow method (NFM)[8], has been used. The NFM is essentially an evaluation process, where the decision maker's preferences are included by means of some constraint-like parameters[8]: indifference, preference, veto thresholds and the relative weights of each objective. A complete description of the NFM and its application to chemical engineering problems are presented in Thibault[16]. The four parameters used for each objective in the NFM are briefly described as follows:

(a) The first parameter gives the relative importance of each objective or criterion *k*, expressed as a relative weight (W_k). In this algorithm, the weights are normalized:

$$\sum_{k=1}^{3} W_k = 1 \tag{37}$$

(b) The second parameter is the indifference threshold (Q_k), which defines the range of variation of the difference between the values of the objective *k* for two solutions for which it is not possible to favour one solution over another for that objective.

(c) The third parameter is the preference threshold (P_k). When the difference between the values of objective *k* for two solutions exceeds the preference threshold, the preference is given to solution with the better objective value.

(d) The fourth parameter is the veto threshold (V_k), which serves to ban a solution relative to another solution because the difference between the values of objective *k* is too high to be tolerated. The solution with the worst objective is banned based on a particular objective, even if the other criteria are very good. The veto threshold can be equally considered as non-preference information.

The three thresholds are defined for each criterion such that:

$$0 \leq Q_k \leq P_k \leq V_k \tag{38}$$

The values of the four NFM parameters used in this investigation are presented in Table 3-3.

Table 3-3 Relative weights (W_k), and indifference (Q_k), preference (P_k) and veto (V_k) thresholds for each objective that are used in the NFM algorithm to rank the entire Pareto domain.

Criterion (*k*)	Relative Weight (W_k)	Threshold Values		
		Q_k	P_k	V_k
Conversion (X)	0.6	0.5	1	3
Productivity (Pro)	0.3	0.002	0.004	0.01
Catalyst weight (W)	0.1	500	1000	4000

By defining ranking parameters (Table 3-3), the NFM algorithm[8] is implemented to rank the entire Pareto domain based on the decision-maker's preferences. The NFM algorithm is briefly described as follows.

Using a pair-wise comparison, the difference $\Delta_k[i,j]$ between of objective *k* for solutions *i* and *j*, the individual concordance index $c_k[i,j]$, the global concordance index C[i,j], and the discordance index $D_k[i,j]$ are calculated by using Eqs. (39)-(42), respectively.

$$\Delta_k[i,j] = F_k(j) - F_k(i) \qquad \begin{cases} i \in [1, M] \\ j \in [1, M] \\ k \in [1, K] \end{cases} \tag{39}$$

$$c_k[i,j] = \begin{cases} 1 & \text{if } \Delta_k[i,j] \le Q_k \\ \dfrac{P_k - \Delta_k[i,j]}{P_k - Q_k} & \text{if } Q_k < \Delta_k[i,j] \le P_k \\ 0 & \text{if } \Delta_k[i,j] > P_k \end{cases} \tag{40}$$

$$C[i,j] = \sum_{k=1}^{K} W_k \cdot c_k[i,j] \qquad \begin{cases} i \in [1, M] \\ j \in [1, M] \end{cases} \tag{41}$$

$$D_k[i,j] = \begin{cases} 0 & \text{if } \Delta_k[i,j] \le P_k \\ \dfrac{\Delta_k[i,j] - P_k}{V_k - P_k} & \text{if } P_k < \Delta_k[i,j] \le V_k \\ 1 & \text{if } \Delta_k[i,j] > V_k \end{cases} \tag{42}$$

Using the global concordance and discordance indices, the relative performance of each pair of Pareto-optimal solutions is finally evaluated by calculating each element of the outranking matrix σ[i,j] by using Eq. (43).

$$\sigma[i,j] = c[i,j]\left(\prod_{k=1}^{K}[1 - (D_k[i,j])^3)\right] \qquad \begin{cases} i \in [1, M] \\ j \in [1, M] \end{cases} \tag{43}$$

Finally, the following equation is used to calculate the score of each solution i. The solution with the highest score is the best solution.

$$\sigma_i = \sum_{j=1}^{M} \sigma[i,j] - \sum_{j=1}^{M} \sigma[j,i] \quad (44)$$

The first term in Eq. (44) evaluates the extent to which solution *i* performs relative to all the other solutions in the Pareto domain, while the second term evaluates the performance of all the other solutions relative to the solution *i*[16]. The solutions are then sorted from highest to lowest according to the ranking score.

In the optimization process, instead of relying on the unique solution of the Pareto domain having the best ranking score, it is desirable to divide the NFM results into zones containing high-ranked, mid-ranked, and low-ranked in order to identify graphically where the optimal region is located[17]. The operating conditions associated with the optimal objective function zone are then candidates to be implemented in the process.

3.6 Results and discussion

In this paper, NSGA-II was used to circumscribe the Pareto domain in view of simultaneously optimizing the conversion, productivity and catalyst weight of an industrial scale sulphur dioxide oxidation reactor. To make this optimization study as comprehensive as possible, a total of eleven case studies or process scenarios were defined and compared. Table 3-4 lists these eleven scenarios.

The design parameters and operating conditions of the SO_2 oxidation packed bed reactor are given in Table 3-1. For all scenarios, the inlet gas feed flow rate was 800 mol/s with a composition of 10 mol% SO_2, 11 mol%O_2, 79 mol% N_2. The inlet pressure of the reactor was set to 1.4 atm. The other important input variables are the inlet temperature and the length of each catalytic packed. The latter two variables for each catalytic bed are under the control of the genetic algorithm in order to circumscribe the Pareto domain for each process configuration.

3.6.1 Various process configuration scenarios

In this section, the eleven different process strategies or scenarios are briefly discussed. The different scenarios of Table 3-4 differ from the number of catalytic beds

used, the addition or not of an intermediate SO_3 absorption column and the optimization procedure. For all scenarios where more than one catalytic bed in series are used, even if not mentioned, a heat exchanger is used to decrease the temperature of the gas mixture prior to entering the next catalytic bed.

Table 3-4 Brief description of the various process scenarios that were optimized in this investigation.

Number	Scenario
1	One catalytic bed
2	Two catalytic beds with global optimization
3	Two catalytic beds with individual bed optimization
4	Three catalytic beds with global optimization
5	Three catalytic beds with individual bed optimization
6	Four catalytic beds with global optimization
7	Four catalytic beds with individual bed optimization
8	Two catalytic beds followed by an intermediate absorption column and two catalytic beds with global optimization
9	Three catalytic beds followed by an intermediate absorption column and a fourth catalytic bed with global optimization
10	Four catalyst beds followed by an intermediate absorption column and a fifth catalytic bed with global optimization
11	Minimum-length catalytic bed where the temperature is adjusted to follow the maximum reaction rate curve

Scenario 1 considered the optimization of only one catalytic bed to determine the optimal solution for comparison purpose with other scenarios that are known to lead to better overall solution. Similarly, scenarios 2 and 3 considered the optimization of two catalytic beds in series while performing a global optimization of the two beds or optimizing the two beds separately, respectively. Scenarios 4 and 5 considered the optimization of three catalytic beds in series while performing a global optimization of the two beds or optimizing the two beds separately, respectively. Scenarios 6 and 7 used identical strategies but for four catalytic beds in series. With these seven scenarios, it was desired to see the progressive change of the three objective functions as the number of

catalytic beds was increased as well as to observe the gain in performance when the global optimization is performed compared to the bed-by-bed optimization.

In scenarios 8 and 9, four catalytic beds in series are used with the incorporation of an adsorption column to remove the SO_3 produced in earlier beds in order to favour additional SO_3 production in subsequent beds[2]. In scenario 8, two catalytic beds are used before the intermediate absorption column and followed by two catalytic beds whereas in scenario 9, three beds are used before and one after the absorption column. Similarly, scenario 10 used an intermediate absorption column after four catalytic beds and a fifth catalytic bed after the intermediate absorption column. Scenarios 8 to 10 are obviously more complex due to the addition of an intermediate absorption column and heat exchangers to decrease the temperature of the gas mixture prior entering the intermediate absorption column and to increase the temperature after the absorption column prior to entering the next catalytic bed. The simplified schematic flowsheets of a single-contact and double-contact processes are shown in Figure 3-6.

Finally, scenario 11 considers the ideal case where the temperature of a unique catalytic bed at any location along the bed is changed such that the rate of reaction is always at its maximum for a given conversion. In other words, the local temperature of the catalytic bed is adjusted to follow the maximum-rate curve illustrated in Figure 3-2. This case is considered to have a point of comparison for the minimum amount of catalyst that would be required to achieve a given conversion.

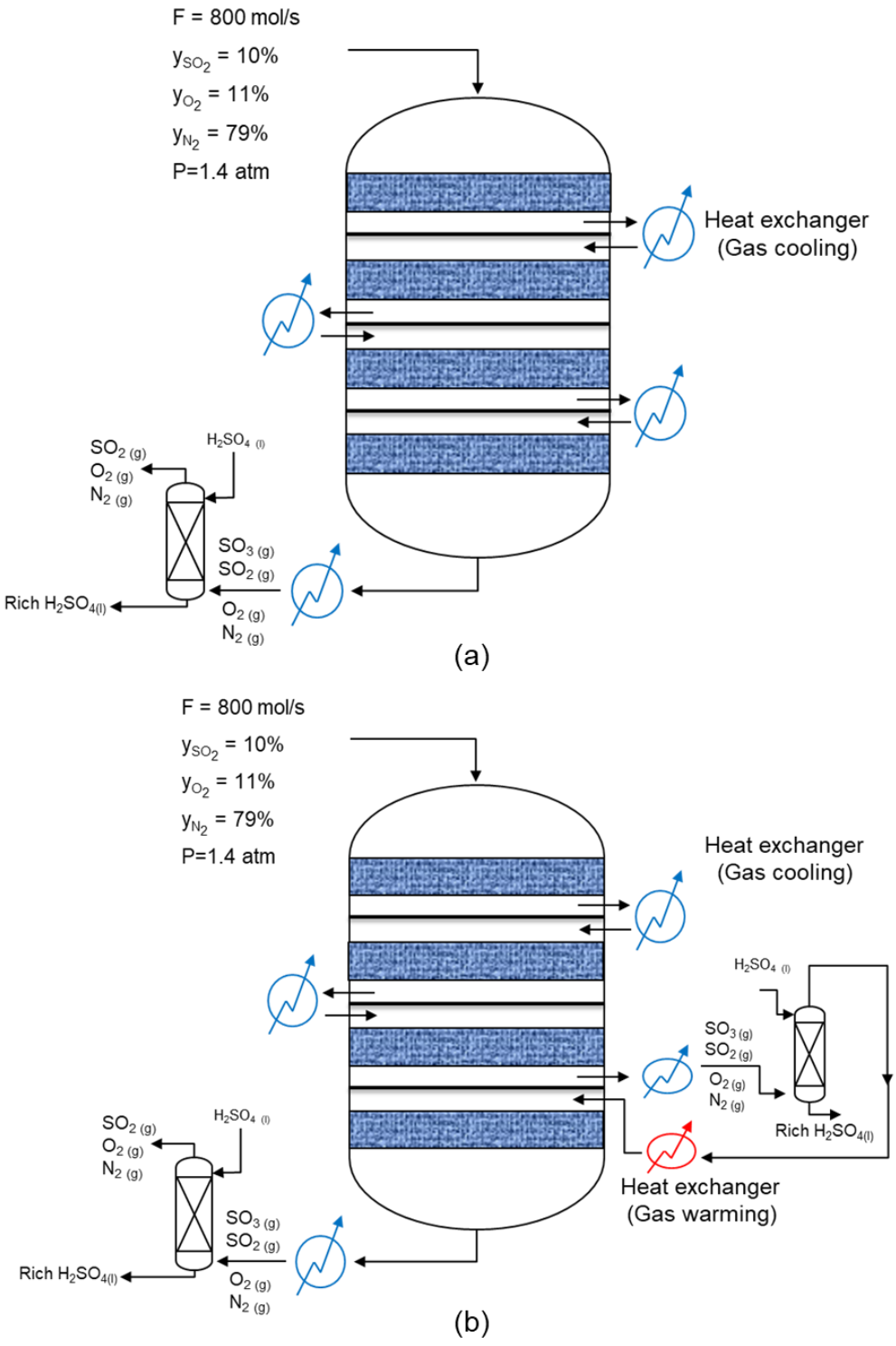

Figure 3-6 Flowsheets of the multiple catalytic bed reactor for the oxidation of SO_2 to SO_3 for (a) the single-contact H_2SO_4 production (Scenario 6) and (b) the double-contact H_2SO_4 production where an intermediate SO_3 absorption column is incorporated between the third and fourth bed (Scenario 9).

3.6.2 Plots of the decision and objective spaces of the Pareto domain

The Pareto domains for all eleven process scenarios using the evolutionary algorithm NSGA-II were circumscribed with the same ensemble of the three objectives (conversion, productivity and catalyst weight) and the corresponding decision variables (inlet temperatures of each catalytic bed and the length of each bed) based on the process scenario considered. Each Pareto domain was ranked with the Net Flow Method to determine the optimal region of operation that has given rise to the best Pareto-optimal solutions based on the preferences of a decision-maker. Instead of having a unique optimal solution, as in classical optimization methods, the distribution of the numerous Pareto-optimal solutions in the solution space offers the opportunity to better understand the underlying interrelationship that exists between the numerous process variables and is able to clearly illustrate the trade-offs that are made when examining the different regions of a Pareto domain.

In this investigation, the eleven Pareto domains had the same shape even though the Pareto front were located at slightly different locations. As a result, only one Pareto domain will be presented and discussed in this paper and only the highest-ranked Pareto-optimal solution for each scenario will be used in the next section to compare the different process strategies.

The results of scenario 6, presented in Figure 3-7, are used to illustrate the shape of the Pareto domain. Results are presented in two-dimensional plots such that the three-dimensional Pareto front is projected onto the two dimensions selected. Results of the ranking by NFM were grouped as follow: the best Pareto-optimal solution followed by the solutions ranked in the best 5%, the next 45% and finally the last 50%.

Figure 3-7 (a)-(c) presents the graphs of the three objective functions of the ranked Pareto domain. Figure 3-7(a) presents the SO_2 conversion exiting the fourth catalytic bed as a function of the productivity. This plot clearly shows the typical compromise that commonly exists between conversion and productivity. An increase in conversion is obtained at the expense of a lower productivity, and vice versa. The NFM parameters were chosen in this investigation to favour a higher conversion because it is required to use as much SO_2 as possible and maintain its concentration low at the end of the process, which needs to be captured and disposed of. However, to further increase the conversion

beyond the highest-ranked solution would decrease significantly the productivity without a significant gain in conversion. Figure 3-7(b) presents the plot of the conversion as a function of the total weight of catalyst for the four beds whereas Figure 3-7(c) presents the plot of the total weight of catalyst as a function of the SO_3 productivity. Figure 3-7(b) clearly illustrates that to reach higher conversion would require an extremely high amount of catalyst and obviously much larger total reactor volume. Figure 3-7(c) shows that higher productivity would be achieved with a low catalyst weight that is a quick production of SO_3 but at a very low conversion. The catalyst weight and the productivity are obviously correlated since the productivity is defined as the number of moles of SO_3 produced per unit time and catalyst weight. It would be possible to use only the conversion and the productivity as objectives, but it was desired to put a small emphasis on the total quantity of catalyst. If the conversion and productivity would be equally desired, the highest-ranked solution would be located closer to the elbow of the curve in Figure 3-7(b) and Figure 3-7(c). In this investigation, more emphasis was placed on conversion, which is also the case industrially.

For the optimization of Scenario 6, there are eight decision variables, namely the inlet temperature and the length of each catalytic bed. The results of the fourth catalytic bed will be presented here as all beds show more or less the same pattern between the inlet temperature and the length of the bed. Figure 3-7(d) shows the plot of the length of the bed as a function of the inlet temperature for the fourth catalytic bed. Because of the exothermic equilibrium reaction, notwithstanding the minimum strike temperature, if the inlet gas temperature is high, the reaction will reach equilibrium rapidly with a relatively low increase in conversion. This higher temperature and the proximity of the equilibrium curve lead to a relatively short length of bed. On the other hand, if the inlet gas temperature is low, the reaction rate will initially be lower and the length of the bed to achieve near-equilibrium will be much longer whereas the conversion will be much higher as shown in Figure 3-2. The nonlinear relationship observed in Figure 3-7(d) is due to the speed of reaction being higher for higher temperature and the shape of the equilibrium conversion curve.

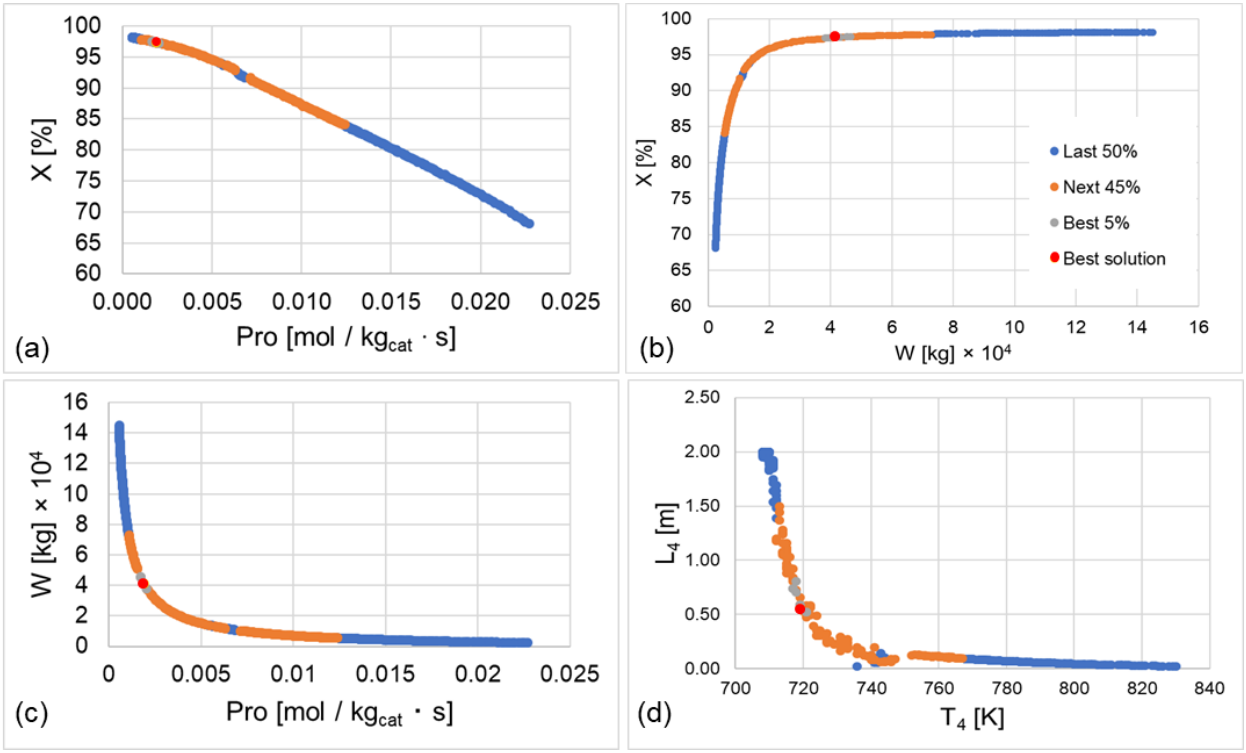

Figure 3-7 Plots of the ranked Pareto domain for the scenario number six where four catalytic beds are considered in single contact method. (a) conversion versus catalyst weight (b) conversion versus productivity (c) catalyst weight versus productivity (d) the two decision variables temperature and length of the last bed.

The ranking of the best 5% of all solutions within the Pareto domain could be affected by relative weight (W_k). With a relative weight of unity for one objective and zero for the other two, one could expect that the optimal zone would shift along the Pareto domain towards the extreme of the favoured criterion. However, this does not occur to the full extent that would be expected because, even though the relative weight for one criterion and its resulting contribution to the concordance index are both zero, the preference and veto thresholds still play the same role with respect to the discordance index. Therefore, the values of the threshold will affect the ranking of a given solution with respect to another when, in a pair-wise comparison, the difference of a given criterion exceeds the preference or the veto thresholds. This sensitivity analysis (results not shown) clearly suggests that the NFM is significantly robust to changes in the relative

weights, and the thresholds play a very important role in the ranking of the Pareto domain[8].

3.6.3 Comparison of various process strategies

Figure 3-8 compares the highest-ranked Pareto-optimal solutions for the conversion, productivity and total catalyst weight for the first ten scenarios described in the previous section. As shown in Figure 3-8(a), the first 7 scenarios simply illustrate the progressive and necessary increase in the number of catalytic beds for the production of SO_3 to achieve a high conversion, going from 70% to over 97%. The use of four catalytic beds in series has been used for many decades industrially to reach the desired conversion. The results of the four catalytic beds are used as a benchmark in this study to investigate the improvements that could result when other strategies are implemented. The target conversion may vary slightly from one industry to the next and, to achieve higher conversion given the thermodynamic limitation of this exothermic equilibrium reaction, one would need to sacrifice the productivity and resort to higher amount of catalyst.

Results of the scenarios 2 to 7 of Figure 3-8(a) were also generated to quantity the loss in performance that would occur if the catalytic beds were optimized individually in sequence rather than being optimized globally with all catalytic beds considered together. As shown in scenarios 3, 5 and 7 for the individual optimization of each bed, the conversion is as expected significantly lower in general than for the global optimization.

Trying to achieve higher conversion by the addition of a fifth catalytic bed did not lead to a significant increase, mainly due to the proximity of the equilibrium curve and the very small existing driving force (results not shown). It is certainly not logical to add a heat exchanger and an extra catalytic bed for a negligible gain in conversion. To achieve higher conversion, the double contact process has been proposed whereby the gas mixture after having achieve a conversion in the vicinity of 90% is passed through a first adsorption column of concentrated sulfuric acid to convert SO_3 to additional sulfuric acid prior to be returned to a catalytic bed to produce more SO_3[18]. The removal of SO_3 from the reacting gas mixture has the advantage to significantly move upward the equilibrium curve as well as to increase the O_2 to SO_2 ratio. The double-contact process has been optimized in this

investigation with three different process flowsheets: (1) two catalytic beds followed by an SO_3 absorption column and two subsequent catalytic beds (Scenario 8), (2) three catalytic beds followed by an absorption column and one subsequent catalytic bed (Scenario 9), and (3) four catalytic beds followed by an absorption column and a fifth catalytic bed (Scenario 10), With these three scenarios, it was possible to achieve a conversion a conversion in excess of 99.5% for the highest-rank Pareto-optimal solutions. It is clear that the double contact process permits to achieve higher conversion and reduce the amount of SO_2 that needs to be discarded. The decision to add an intermediate absorption column would be decided on an economical and environment point of view.

Figure 3-8 (b) and (c) present the values of the productivity and catalyst weight for the highest-ranked Pareto-optimal solutions associated to the different scenarios. These two objectives are correlated since an increase in the catalyst weight leads to a decrease in productivity as the latter is defined as moles of SO_3 produced per second and per kilogram of catalyst. It is clear that to achieve a higher conversion, a much larger weight of catalyst is required and a much lower productivity is obtained. In this investigation, a greater importance has been given to conversion as it is favoured in industrial production. Nevertheless, the ranking algorithm (NFM) attempts to strike a compromise between the three objectives whereby a high conversion is achieved but without using an excessive amount of catalyst. It is interesting to note that the three scenarios (8, 9 and10) involving the double-contact process have identical productivity and catalyst weight. This is understandable since the process is limited by the upper limit of conversion, which was nearly reached with these three scenarios.

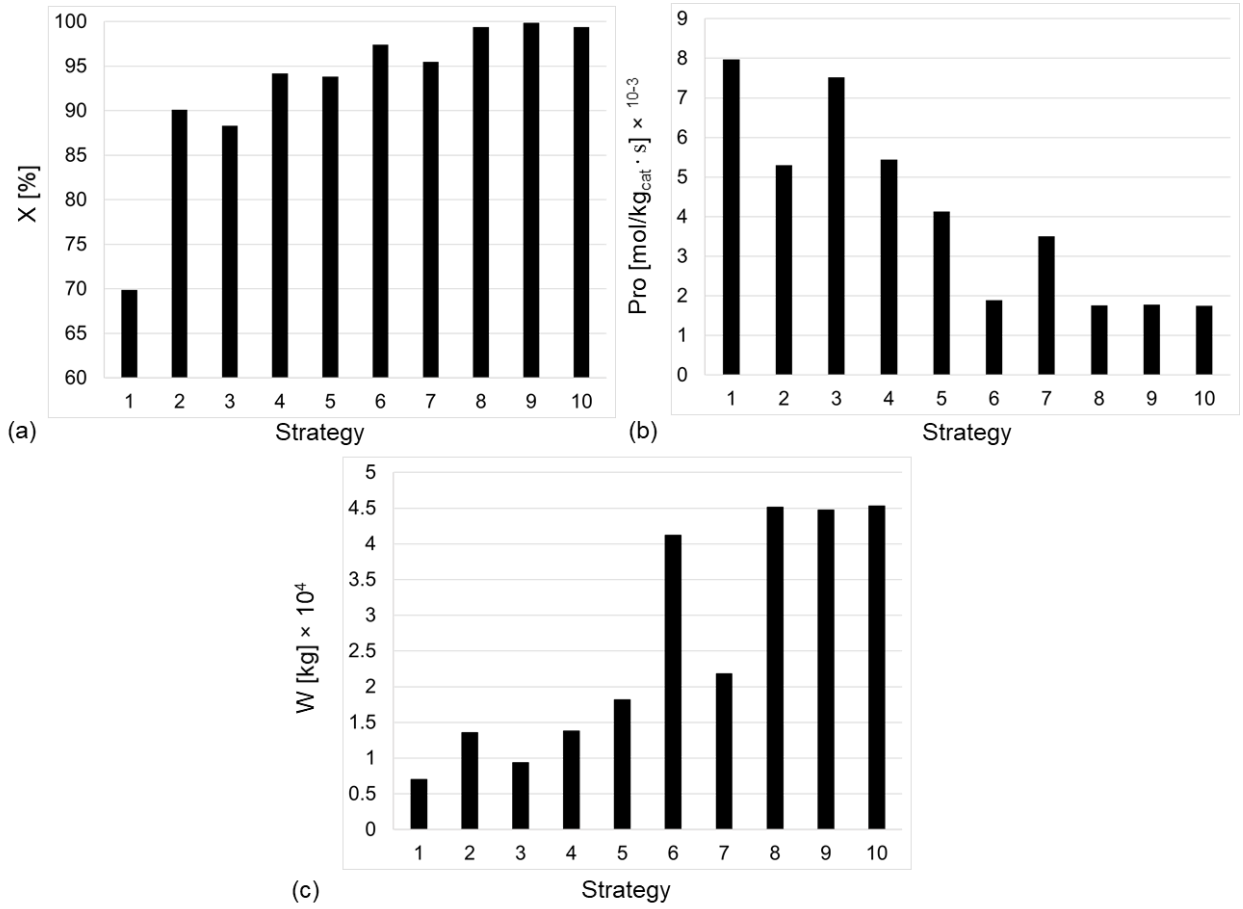

Figure 3-8 Comparison of the optimal values for three objectives between various scenarios that is defined in Table 3-4 based on the number of catalytic beds and arrangement of the beds. (a) comparing the conversion (b) comparing the productivity (c) comparing the catalyst weight.

3.6.4 Minimum length

It is always interesting in an optimization study to determine limiting values of objectives even it they cannot be achieved in practice. In this investigation, it was decided to determine what would be the minimum length (or catalyst weight) to reach a conversion equal to the conversion that was obtained with four catalytic beds (Scenario 6). In this case, the minimum length of a unique bed would be achieved when the temperature is adjusted at all locations along the packed bed such that the reaction rate is always at its maximum value. In other words, conversion-temperature profile needs to follow the

maximum-rate curve described in Figure 3-2. A series of simulations were performed to determine the minimum length of the bed over a range of inlet reactor temperatures (Scenario 11). For a given inlet temperature, the temperature was kept constant until the conversion at which the maximum reaction rate was reached. Thereafter, the temperature was adjusted to follow the constant-rate curve. Results of this study are presented in Figure 3-9.

Results of Figure 3-9 show that for smaller inlet temperatures, the length of the variable-temperature catalytic bed is relatively high because a longer portion of the bed is maintained at the inlet temperature where the reaction rate is lower than its optimal value for a given conversion. As the temperature increases, the length of the bed decreases significantly. For comparison, the total length of the four catalytic bed of Scenario 6 has been plotted on Figure 3-9, which shows that the variable temperature catalytic bed would start to show better performance when the inlet temperature exceeds 790 K. This comparison is interesting because it shows that the length of the four-bed catalytic reactor (Scenario 6) is not significantly different than the best that could be obtained with the large adiabatic reactor (about 5% difference in the best case for the same conversion).

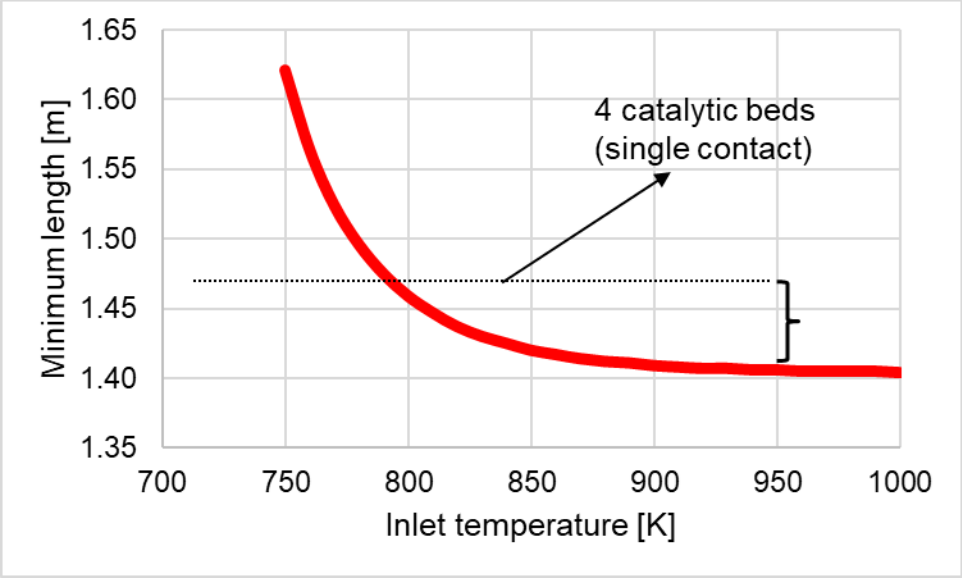

Figure 3-9 Plot of the minimum length of the catalytic bed as a function of inlet temperature (Scenario 11), which is compared with the length of bed of the four catalytic beds for the same optimal conversion.

Conclusions

This study has considered the multi-objective optimization of the sulphur dioxide oxidation to the sulphur trioxide. The optimization of this process considered a series of input or decision variables (temperature and length of each bed) and three process objectives (SO_2 conversion, SO_3 productivity and catalyst weight). A series of scenarios or process strategies were defined and optimized, which consisted in each case to circumscribe the Pareto domain using a genetic algorithm. All Pareto-optimal solutions were then ranked using the Net Flow method where the knowledge and preferences of a decision-maker were used. The knowledge of the decision-maker was encapsulated into a relative weight of each objective along their respective indifference, preference and veto thresholds.

This analysis allowed determining the operating conditions of each scenario that led to the best trade-off among all objectives. The highest SO_2 conversion was obtained in a double-contact process. Indeed, when the SO_2 conversion reaches approximately 90%, it is advantageous to use an intermediate absorption column to recreate favourable conditions for higher SO_2 conversion. On the other hand, the four catalytic bed reactor, commonly used industrially, still provides a very good conversion which is nearly operating with the minimum length of bed that is ideally achievable. The next step in this investigation is to perform the global optimization of the sulphuric acid process which would include the major process equipment.

Acknowledgments

The authors gratefully acknowledge the financial support for this project provided by the Natural Science and Engineering Research Council of Canada.

Abbreviations

MOO	Multi-objective optimization
NFM	Net Flow method
NSGA	Non-Dominated Sorting Genetic Algorithm

Nomenclature

ε	Void fraction
μ	Viscosity [Pa · s]
$\emptyset$	Wilke's coefficient
ρ_b	Bed density [kg/m^3]
ρ_f	Fluid Gas density [kg/m^3]
ΔH_R	Heat of reaction [J/mol]
A	The reactor area [m^2]
C_p	Molar heat capacity [J/mol·K]
$C_{p,\ Mix}$	Molar heat capacity of gas mixture [J/mol K]
D_{bed}	Bed diameter [m]
D_p	Particle diameter [m]
F	Molar flow rate [mol/s]
F_i	Molar flow rate of component [mol/s]
K	Number of objectives
k_1	Rate coefficient for reaction [kmol/kg$_{cat}$ · atm · s]
K_2	Rate coefficient for reaction [atm^{-1}]
K_3	Rate coefficient for reaction [atm^{-1}]
K_P	Equilibrium constant [atm$^{-0.5}$]
L	Length of bed [m]
M	The number of solutions in the Pareto domain
M_w	Molecular weight [kg/kmol]
P	Total pressure [atm]

p_i	Partial pressure [atm]
P_k	Preference threshold for criterion k in NFM algorithm
Pro	Productivity [mole/kg_{cat} · s]
Q_k	Indifference threshold for criterion k in NFM algorithm
R	Gas constant [8.314 J/mol · K]
r_{SO_2}	Rate of reaction [kmol/kg_{cat} · s]
T	Temperature [K]
T_{ref}	Reference temperature [K]
u	Superficial gas velocity [m/s]
V_k	Veto threshold for criterion k in NFM algorithm
W	Catalyst weight [kg]
W_k	Weight for each objective criterion
X	Conversion [fraction or %]
y_i	Mole fraction [fraction or %]

Appendices

Appendix A– Heat capacity

According to Fogler[18], the heat capacity of each species at temperature (T) is frequently expressed as a quadratic function of temperature:

$$C_p = A + B \times T + C \times T^2 \quad (45)$$

here A, B, C are coefficients that are given in the following Table A.1.

To approximate the specific heat capacity of a mixture with an infinite number of components when the mole and specific heat capacity of each species is known, the rule of mixtures calculator is used:

$$C_{p,mix} = \sum_{i=1}^{\text{number of species}} y_i \times C_{p,i} \quad (46)$$

where y_i is the mole fraction of species i

Table 3-5A Heat capacity coefficients

Component	SO_2	SO_3	O_2	N_2
A (J/mol. K)	30.178	35.634	23.995	26.159
B (J/mol. K^2)	42.452×10^{-3}	71.722×10^{-3}	17.507×10^{-3}	6.615×10^{-3}
C (J/mol. K^3)	-18.218×10^{-6}	-31.539×10^{-6}	-6.628×10^{-6}	-2.889×10^{-6}

Appendix B- Heat of reaction

In this study, where heat capacities are strong functions of temperature over a wide temperature range. Under these conditions, the heat of reaction of the SO_2 oxidation is calculated from the following equation[18]:

$$\Delta H_R = \Delta H_R(\text{at the } T_{ref}) - 6.54 \times (T - T_{ref}) + \frac{0.0205}{2} \times \left(T^2 - T_{ref}^2\right) - \frac{10.007 \times 10^6}{3} \times (T^3 - T_{ref}^3) \quad (47)$$

the heat of reaction at a reference temperature, 700 K, is -98787.5 kJ/kmol.

Appendix C- Gas viscosity

Viscosity in gases arises principally from the molecular diffusion that transports momentum between layers of flow[19]. The kinetic theory of gases allows accurate prediction of the behaviour of gaseous viscosity. Within the regime where the theory is applicable: viscosity is independent of pressure and viscosity increases as temperature increases. To estimate the dynamic viscosity of an ideal gas as a function of the temperature, Unisim is used for the range temperature of 500 < T < 900 [K]:

$$\begin{aligned}
\mu_{SO_2} &= 4.67 \times 10^{-8}\,T - 2.23 \times 10^{-6} \quad [Pa.s] \\
\mu_{SO_3} &= 5.68 \times 10^{-8}\,T - 9.09 \times 10^{-6} \quad [Pa.s] \\
\mu_{O_2} &= 4.12 \times 10^{-8}\,T - 5.79 \times 10^{-6} \quad [Pa.s] \\
\mu_{N_2} &= 4.34 \times 10^{-8}\,T - 8.99 \times 10^{-6} \quad [Pa.s]
\end{aligned} \tag{48}$$

Wike[20] chose to use an equation derived from the simple kinetic theory that is easily extended to multi-component systems. It requires the evaluation of a complicated coefficient ($\emptyset_{ij}$) for each pair of components in a mixture. The evaluation requires only the viscosity and the molecular weights (Mw_j) of individual components:

$$\emptyset_{ij} = \frac{\left[1 + \left(\frac{\mu_i}{\mu_j}\right)^{0.5} \cdot \left(\frac{Mw_j}{M_i}\right)^{0.25}\right]^2}{\frac{4}{\sqrt{2}}\left[1 + \frac{Mw_i}{Mw_j}\right]^{0.5}} \tag{49}$$

these coefficients are then used with the mole fraction in the calculation of the viscosity of the mixture:

$$\mu_{Mix} = \sum_i \frac{y_i \mu_i}{y_i + \sum_{j \neq i} y_j \emptyset_{ij}} \tag{50}$$

References

1. Arkema Inc. Sulfuric Acid Safety data sheet. https://www.arkema-americas.com/en/ (2004).
2. King, M. J., Davenport, W. G. & Moats, M. S. Overview. in Sulfuric Acid Manufacture Elsevier, pp 1–9 (2013).
3. Kiss, A., S.Bildea, C. & Grievink, J. Dynamic modeling and process optimization of an industrial sulfuric acid plant. Chem. Eng. J. 158, pp 241–249 (2010).
4. King, M. J., Davenport, W. G. & Moats, M. S. Catalytic oxidation of SO_2 to SO_3. in Sulfuric Acid Manufacture. Elsevier, pp 73–90 (2013).
5. Sultana, S. T. Simulation and optimization of sulfuric acid plant. Bangladesh University of Engineering and Technology, pp 34-38 (2012).
6. Sørensen, P. A., Møllerhøj, M. & Christensen, K. A. New dynamic models for simulation of industrial SO_2 oxidation reactors and wet gas sulfuric acid plants. Chem. Eng. J. 278, pp 421–429 (2015).
7. Nouri, H. & Ouederni, A. Experimental and modeling study of sulfur dioxide oxidation in packed-bed tubular reactor. Int. J. Innov. Appl. Stud. **3**, pp 1045–1052 (2013).
8. Thibault, J. Net flow and rough sets: Two methods for ranking the pareto domain. in Multi-Objective Optimization: Techniques and Applications in Chemical Engineering pp 199–246 (2016).
9. Clark, D., Vavere, A. & R. Horne, J. Using Super Cesium Catalyst to Increase Sulfuric Acid Production. AIChE Conv. Clear. pp 1–6 (2007).
10. Collina, A., Corbetta, D., and Cappelli, A., "Use of Computers in the Design of Chemical Plants", in Proc. Eur. Symp, Firenze, pp 329 (1971).
11. Eklund, R. B, Dissertation in the Manufacture of Sulfuric, Royal Institute of Technology, Stockholm, pp. 166–168. (1956)
12. Calderbank P H. The mechanism of the catalytic oxidation of sulphur dioxide with a commercial vanadium catalyst: A kinetic study. J. App. Chem., pp 482-492.(1952)
13. Villadsen, J. & Livbjerg, H. Kinetics and effectiveness factor for SO2 oxidation on an industrial vanadium catalyst. Chem. Eng. Sci. 27, pp 21–38 (1972).

14. Deb, K., Pratap, A., Agarwal, S. & Meyarivan, T. A fast and elitist multi-objective genetic algorithm:NSGAII. IEEE, pp182–197 (2002).
15. Deb, H. G. B. and K. On Self-Adaptive Features in Real-Parameter Evolutionary Algorithm. IEEE Trans. Evol. Comput. 121, pp 250–270 (2001).
16. Thibault, J., Lanouette, R., Fonteix, C. & Kiss, L. N. Multicriteria Optimization of a High-Yield Pulping Process. Can. J. Chem. Eng. 80, pp 897–902 (2008).
17. Thibault, J. et al. Multicriteria optimization of a high yield pulping process with rough sets. Chem. Eng. Sci. 58, pp 203–213 (2003).
18. Mars, P. & Maessen, J. G. H. The mechanism and the kinetics of sulfur dioxide oxidation on catalysts containing vanadium and alkali oxides. J. Catal. 10, 1–12 (1968).
19. Dussauge, A. J. smit. and J.-P. Turbulent shear layers in supersonic Flow. Springer Science and Business Media. Springer Science and Business Media, pp 1689-1699(2006).
20. Davidson, T. A Simple and Accurate Method for Calculating Viscosity of Gaseous Mixtures., McGraw-Hill, pp 741 (1993).

Chapter 4. Conclusions and recommendations

This thesis has mainly aimed much of its attention at the modelling and optimization of the sulphur dioxide oxidation to sulphur trioxide, which is the most critical step in sulphuric acid production process. First, the attention was focussed in identifying the most appropriate kinetic rate equation that was able to best represent the available experimental data in the temperature range of interest. Second, this thesis was aimed to determine the optimal operating conditions of the multi-bed catalytic reactor in which the oxidation of SO_2 to SO_3 is taking place in order to best satisfy some conflicting objectives in the eye of a decision-maker.

In Chapter 2, after providing a brief background on the development and applications of sulphuric acid production, more emphasis was placed on the catalytic oxidation of SO_2 to SO_3. The various parameters that can affect the equilibrium SO_2 oxidation such as the temperature, the pressure and the concentration of reacting mixture were studied. The equilibrium SO_2 conversion can be improved by increasing partial pressure of some reactants (SO_2, O_2) and operating pressure. Also, a lower inlet temperature, provided it is hot enough to reach the auto-ignition temperature to have a self-sustaining catalytic oxidation (~415°C-425°C), allows to achieve a higher conversion in each bed. To study the SO_2 oxidation which takes place along a multi-bed catalytic reactor and taking into account all the above-mentioned parameters, it is essential to find a proper kinetic model. In this regard, through a literature review, some kinetic models, based on the vanadium pentoxide catalyst commonly used industrially, were identified and tested as to their ability to predict the SO_2 oxidation experimental data over a wide range of operating conditions. The retained kinetic rate equation, based on the minimum residual sum squares between the predicted and experimental data, was the model proposed by Collina et al., This model best represented the experimental data for a feed gas composition of 10 mol% SO_2, 11 mol%O_2 and at a pressure slightly above atmospheric (~ 1.4 atm).

In chapter 3, a systematic methodology was presented to perform the multi-objective optimization of the SO_2 oxidation to SO_3 in multi-bed catalytic packed bed reactor. The optimization process considered a number of decision or input variables (temperature and length of each bed) and three partially conflicting process outputs or objectives (the SO_2 conversion, the SO_3 productivity and the catalyst weight). Eleven cases, considering the number of catalytic beds and the presence or not of an intermediate SO_3 absorption column, were studied and optimized for the catalytic packed bed reactor. Results, as expected, showed that the optimization must be performed on the overall process rather than on individual components. Moreover, with the same number of catalytic beds, the incorporation of an intermediate SO_3 absorption column showed higher conversion in comparison with the process without the intermediate column. However, the higher conversion is achieved at the expense of higher operating costs. Finally, results showed that the optimal bed length, obtained when following the maximum reaction rate curve, was nearly reached (within 5%) with the process comprised of four catalytic beds.

The results from this work highlight the clear benefits of employing a multi-objective optimization algorithm in a process involving numerous conflicting objectives. In addition to providing the set of optimal solutions for every process strategies and reactor configurations, the results are an invaluable source of information that could be used in choosing a proper strategy as they allow the decision maker to readily visualize the inherent interrelationship between the different process variables.

Based on the results obtained in this study, it would be interesting in the future to consider the operating and capital costs of the sulphuric acid manufacturing process as objective functions to decide where lie the optimal operating conditions, and if it is different than considering only technical process objectives. This analysis must also go beyond the multi-bed catalytic reactor but must also include other process equipment such as heat exchangers and absorption columns in the optimization process to fully cover all aspects of sulphuric acid production. Moreover, research was done for the steady-state models, where dynamic changes were not considered. Further research could be done in dynamic multi-objective optimization as the decision variables will also vary according to time. Last but not least, it would be useful to aim to resort to machine learning to

recognize mathematical patterns in the process, participants will develop an intuition for which problems are solvable using standard numerical modelling techniques and gain the knowledge and skills to then solve them.